



**Politecnico
di Torino**

Politecnico di Torino

Department of Environment, Land and Infrastructure
Engineering

**Master of Science in Georesources and Geoenergy
Engineering**

A.Y 2024/2025

**Static and dynamic model of a real hydrocarbon
reservoir for future conversion to underground H₂
storage**

Supervisors:

Prof. Vera Rocca

Prof. Christoforos Benetatos

Candidate:

Georges El Achkar

Abstract

Hydrogen is emerging as a crucial energy carrier in the transition toward a sustainable and low-carbon energy system, and its large-scale storage is essential for balancing supply and demand, particularly when integrating renewable energy sources. Among the various storage solutions, hydrogen storage in depleted reservoirs presents a promising solution for large-scale energy storage, leveraging existing infrastructure and proven containment integrity. This study assesses the feasibility of underground hydrogen storage in the Norne field, focusing on static and dynamic modeling to evaluate storage efficiency, pressure stability, and recovery performance. A static model, Performed on Petrel, characterizes the reservoir's geological and petrophysical properties, while an analysis of production history provides insight into past depletion and pressure behavior. Dynamic simulations, conducted using ECLIPSE® 100, model hydrogen injection as a solvent in its critical state and evaluate three storage scenarios within the gas cap using existing wells. This study highlights the importance of well configuration, injection strategies, and pressure management in optimizing UHS in depleted reservoirs, contributing to the development of large-scale UHS solutions and supporting the broader adoption of hydrogen as a key component of the future energy landscape.

Table of Contents

Abstract	1
Scope of Work.....	6
I. Introduction	8
II. UHS in Depleted Hydrocarbon Reservoirs Overview	11
1. Site Selection for UHS Projects:	12
2. Underground Storage Types.....	13
2.1. Salt Caverns.....	13
2.2. Depleted Gas and Oil Reservoirs.....	14
2.3. Saline Aquifer Formations	16
3. Trapping Mechanisms.....	16
3.1. Structural Trapping	16
3.2. Capillary Trapping	17
3.3. Solubility Trapping	18
3.4. Mineral Trapping	18
4. Rock-Fluid Properties	19
4.1. Interfacial Tension	19
4.2. Wettability and Contact Angle.....	21
4.3. Capillary Pressure	23
4.4. Relative Permeability Hysteresis	24
5. Diffusivity	26
6. Potential Risks.....	27
6.1. Microbial Reactions	27
6.2. Geochemical Reactions	29
6.3. Physical Risks.....	30
6.4. Caprock Integrity	31
7. Underground Hydrogen Behavior	33
8. Case Studies	36
III. Model Characterization	38
1. Numerical Simulation and Modeling	38
2. Static Model and Geological Description	39
3. Dynamic model	41
3.1. Reservoir Injection, Production and Pressure History	43
3.2. Forecast Scenarios for H ₂ Storage	49

3.3. Results and Discussion.....	52
IV. Conclusion.....	61
References	63

List of Figures

Figure 1 Hydrogen use by sector [1].....	8
Figure 2 Salt Cavern [53]	14
Figure 3 Depleted hydrocarbon reservoir [11]	15
Figure 4 Structural trapping by caprock [13]	17
Figure 5 H ₂ Trapping mechanisms overview [16]	19
Figure 6 Effect of pressure on the IFT of H ₂ -brine system [19]	20
Figure 7 Salinity effect on IFT in H ₂ -brine system [19].....	21
Figure 8 Brine contact angles on the pure quartz surface in H ₂ -atmosphere as a function of Pressure and Temperature [21]	23
Figure 9 Brine contact angles on the quartz surface in the H ₂ -atmosphere as function of stearic acid concentration [21].....	23
Figure 10 Capillary pressure hysteresis curves [23]	24
Figure 11 Relative permeability hysteresis curves: Displacement direction dependent (left), Saturation history dependent (right) [53]	25
Figure 12 H ₂ diffusivity for hydrocarbon fluids as a function of temperature and pressure [26]..	26
Figure 13 H ₂ diffusivity in brine as a function of temperature and pressure [26]	26
Figure 14 Kinetic dissolution of individual mineral phase of quartz-rich caprock [40]	32
Figure 15 Diffusion coefficient comparison computed for H ₂ and CH ₄ from wet caprock [42]...	32
Figure 16 H ₂ density in function of Pressure and Temperature [45].....	34
Figure 17 H ₂ viscosity in function of Pressure and Temperature [46]	35
Figure 18 map representing the Norne field location	39
Figure 19 3D view of the grid.....	40
Figure 20 Cumulative Field Gas Production Plot	44
Figure 21 Field Pressure Plot.....	44
Figure 22 Cumulative Field oil Production Plot	45
Figure 23 Cumulative Water Production Plot.....	45
Figure 24 Cumulative Water Injection Plot.....	47
Figure 25 Cumulative Gas Injection Plot	47
Figure 26 Well distribution map.	49
Figure 27 Gas Injection Rates for different scenarios during infilling and storage cycles	51
Figure 28 Gas Production Rate variations for different scenarios during withdrawal phases.	51
Figure 29 Gas cap regional pressure profile for different storage cases.	52
Figure 30 Hydrogen in Place Plot.....	55
Figure 31 Cumulative H ₂ Production Plot.....	57
Figure 32 Base Case 3D Grid After Injection.....	58
Figure 33 Case 2 3D Grid After Injection	58
Figure 34 Case 1 3D Grid After Injection	58
Figure 35 Base Case 3D Grid After Injection.....	59
Figure 36 Case 1 3D Grid After Injection	59
Figure 37 Case 2 3D Grid After Injection	59

List of Tables

Table 1 Classification of H ₂ Based on Production Methods and Environmental Impact [4]	9
Table 2 H ₂ Supercritical State Conditions [43]	33
Table 3 Reservoir properties	41
Table 4 Summary of Production and Injection History	48
Table 5 Summary of Injection and Production Strategies	50
Table 6 Comparison of Pressure Behavior Across Different Cases	54
Table 7 Hydrogen Working Gas, Injected Gas, and Recovery Efficiency Across Cycles	56

Scope of Work

This study investigates the viability of utilizing the depleted Norne Field in the Norwegian Sea for large-scale underground hydrogen storage as a means of supporting the transition to a sustainable energy system. By adopting a multidisciplinary approach, this study combines geological characterization with dynamic reservoir simulations to assess the field's capacity for hydrogen injection, withdrawal and containment. A 3D numerical simulation approach is essential to capture the primary trapping mechanisms governing hydrogen storage and retrieval. The approach taken aligns with the predominant trapping mechanisms expected in this, namely structural, stratigraphic, and residual trapping, which are widely recognized in literature as the key factors influencing hydrogen retention in depleted reservoirs.

Moreover, given the cyclic nature of underground hydrogen storage, hysteresis effects were explicitly accounted for using Killough's hysteresis model for both the wetting and non-wetting phases, as this approach enables a more realistic prediction.

The work incorporated:

- **Static Model Refinement:** Review and refinement of the existing static reservoir model from the Open Porous Media (OPM) initiative, representing the field's compartmentalized structure and petrophysical properties.
- **Dynamic Simulation:** The dynamic simulation of hydrogen storage in the Norne field was conducted using the ECLIPSE® 100 simulator, as the publicly available Norne model, was originally developed in this framework. Given the limitations of the black oil model, the Solvent option in ECLIPSE® 100 was employed to introduce hydrogen as a distinct dry

gas phase. Its properties were derived from literature sources to ensure an accurate representation of hydrogen behavior within the reservoir. This approach enabled differentiation between both the injected natural gas and hydrogen.

- **Comparative Analysis:** Three hydrogen storage scenarios were evaluated over a 10-year period characterized by an infilling phase, followed by 4 storage cycles and ending with a prolonged withdrawal period, where hydrogen is injected as a solvent alongside natural gas that acts as a cushion gas. The already existing wells and infrastructure in the Norne field were utilized, and the simulations aimed to assess the efficiency and feasibility of underground hydrogen storage by employing different well configurations with different injection and withdrawal strategies.
- **Results and Discussion:** By analyzing several reservoir performance indicators such as field pressure evolution, hydrogen saturation distribution, recovery efficiency, and storage stability, the three cases were analyzed and compared. The analysis identifies key advantages and limitations for each case, offering insights into optimizing hydrogen storage in depleted reservoirs.

This research enhances the understanding of underground hydrogen storage viability, providing a foundation for future studies utilizing compositional simulators to achieve a more detailed representation of underground hydrogen behavior and storage.

I. Introduction

Hydrogen has emerged as a cornerstone of the global transition to sustainable energy systems and due to its unique properties and diverse applications, its global demand in 2023 increased by 2.5% compared to 2022, reaching a total of 97 million metric tons (Mt) and expecting to reach a total of 145 million metric tons (Mt) by 2030, as shown in (Fig.1) [1]. As the simplest and most abundant element, hydrogen has immense potential as a clean and efficient energy carrier. Hydrogen only emits water vapor when used in fuel cells or combustion processes, making it an environmentally friendly alternative to fossil fuels. However, since it requires more energy to produce than it yields when employed, hydrogen is not considered as a main energy source but as an efficient energy carrier because of its transporting and storing capabilities. [3]

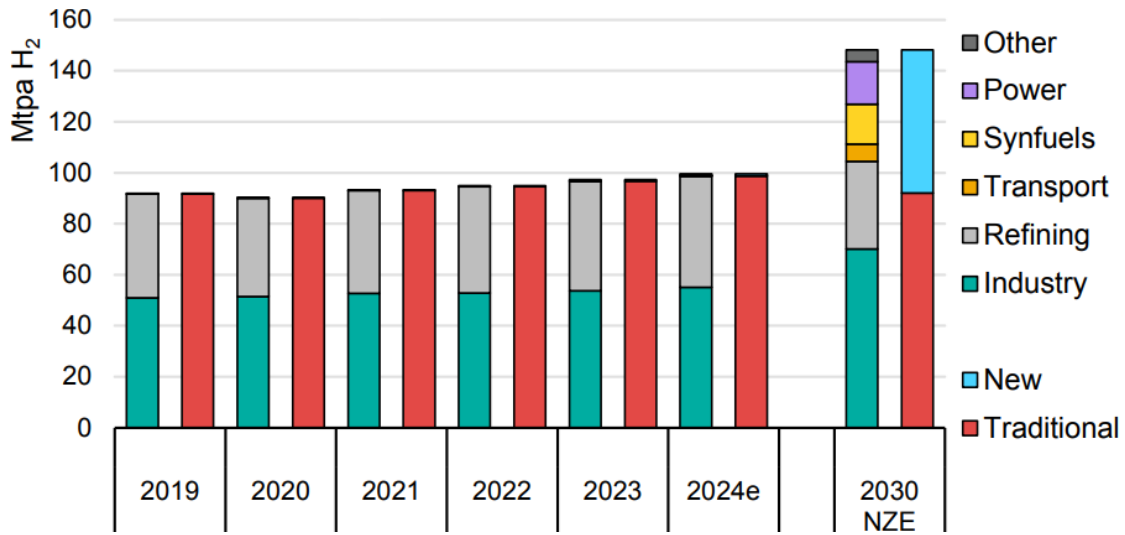


Figure 1 Hydrogen use by sector [1]

Moreover, it is gaining significant attention for its potential to achieve net-zero emissions with the ability to integrate into multiple sectors ranging from transportation to electricity generation and storage, making it crucial for current and future energy systems. For instance, it

can provide heat for industrial processes, and store excess renewable energy for later use, ensuring a stable energy supply depending on seasonal changes [2][3]. Furthermore, hydrogen can be produced from various resources, including natural gas, coal, biomass, and renewable energy through water electrolysis. Based on its production methods, hydrogen can be classified into different types, each with distinct environmental impacts [4].

Table 1 Classification of H₂ Based on Production Methods and Environmental Impact [4]

Type of Hydrogen	Production Method	Environmental Impact
<i>Green Hydrogen</i>	Produced by electrolysis of water using renewable energy sources (wind, solar, hydro)	Zero direct CO ₂ emissions, cleanest option
<i>Turquoise Hydrogen</i>	Produced through pyrolysis of methane, generating solid carbon	Emerging technology, potential for low CO ₂ emissions
<i>Blue Hydrogen</i>	Produced via SMR with carbon capture and storage (CCS)	Reduced CO ₂ emissions, more sustainable than grey hydrogen
<i>Grey Hydrogen</i>	Produced through steam methane reforming (SMR) from natural gas	High CO ₂ emissions, less environmentally friendly

Despite these advantages, one of the fundamental challenges in adoption of hydrogen lies in its storage because of its very low volumetric energy density, which is why it requires advanced storage methods to ensure it can be utilized at scale. Consequently, conventional approaches such as high-pressure tanks or cryogenic systems are effective for small-scale or mobile applications but become impractical for the large volumes required to support energy grids or industrial operations. As a result, this limitation has led to the exploration of underground hydrogen storage as a solution that leverages geological formations to store hydrogen efficiently and at scale. By

addressing the storage challenge, hydrogen can truly fulfill its potential as a cornerstone of the clean energy transition [4].

Underground hydrogen storage is a highly efficient and reliable solution for large-scale, long-term hydrogen storage, leveraging geological formations such as salt caverns, depleted reservoirs, and aquifers. From a structural point of view, salt caverns are the most reliable, while depleted hydrocarbon reservoirs make more sense from an operational and financial standpoint. Saline aquifers and depleted hydrocarbon reservoirs, particularly gas reservoirs, have been extensively explored for large-scale and long-term hydrogen storage since salt caverns may not be readily accessible for hydrogen storage in many parts of the globe. Nonetheless, these formations offer vast storage capacities, far exceeding the limitations of above-ground methods like high-pressure tanks or cryogenic systems, making UHS particularly suitable for seasonal energy storage. Furthermore, it is also cost-effective in the long run, as the scalability of geological formations significantly reduces storage costs per unit of hydrogen compared to surface-based options [5]. Safety is another significant advantage, as UHS minimizes the risk of leaks and external hazards by securely storing hydrogen in deep permeable reservoirs with thick, impermeable caprock layers that act as natural seals, ensuring that hydrogen remains contained deep underground.

All things considered, UHS integrates seamlessly with renewable energy systems, storing surplus hydrogen produced during peak energy generation and supplying it during periods of high demand or low renewable output. This combination of scalability, cost-efficiency, safety, and flexibility positions UHS as a base for the future hydrogen economy. [6]

II. UHS in Depleted Hydrocarbon Reservoirs

Overview

Underground hydrogen storage (UHS) in depleted hydrocarbon reservoirs presents a viable solution for large-scale hydrogen containment and extraction. These reservoirs, which previously held oil or natural gas, possess favorable geological characteristics, such as porous and permeable rock formations with established caprock seals that prevent hydrogen migration. Usually, working gas, i.e. H_2 , is injected alongside a gas cushion like CH_4 which is meant to be kept in storage reservoirs as permanent inventory to sustain sufficient deliverability rates and pressure during withdrawal periods. Furthermore, the usage of a hydrogen and cushion gas mixture is also partly because of legal regulations that limit the maximum allowable H_2 fraction present in gas mixtures. [50]

The advantages of utilizing depleted reservoirs include their large storage capacity, making them suitable for cyclical storage, and the availability of pre-existing infrastructure, such as wells and pipelines, which reduces development costs. Furthermore, UHS is characterized by a cyclic injection and withdrawal strategy, where H_2 is typically injected for a period of 6 to 7 months, and withdrawn for a period of 5 to 6 months a year. This cyclic phase is typically preceded by an infilling phase and proceeded by a prolonged withdrawal phase [51]. The different mechanisms, benefits and risks associated with the UHS process will be examined, beginning with the various factors that need to be considered when selecting a suitable candidate site.

1. Site Selection for UHS Projects:

To qualify as an appropriate site for underground hydrogen storage, geological formation must meet several essential conditions. These conditions ensure the storage system's efficiency, safety, and economic viability while maintaining the integrity of the stored hydrogen over time. This list encompasses the general necessary criteria required, as more details will follow in the rest of the paper.

- **Permeable Reservoir:** The storage formation must consist of porous and permeable reservoir rock, such as sandstone with a minimum recommended porosity and permeability of 10% and 100 mD, respectively [7]. This facilitates the injection and extraction of hydrogen since both high permeability and porosity ensure the efficient movement of hydrogen within the reservoir, making the storage and withdrawal processes practical and effective.
- **Impermeable Caprock:** A critical feature of a suitable storage site is the presence of a thick, impermeable caprock with permeability less than 0.1 mD [8] such as shale or salt. This caprock acts as a natural seal, preventing hydrogen from escaping to the surface or migrating into surrounding formations. Further, the integrity of the caprock is essential for long-term containment.
- **Adequate Storage Capacity:** The formation must have sufficient pore volume to accommodate the required amount of hydrogen as large storage capacities are particularly important for seasonal storage. [9]
- **Structural Integrity:** The geological structure must demonstrate stability under the pressures associated with hydrogen storage. Features such as anticlines or fault-sealed traps

enhance the reservoir's ability to contain hydrogen securely and withstand potential stress without failure.

- **Depth, Pressure and Temperature:** The site should be located at a depth where the pressure and temperature conditions are suitable for hydrogen storage, ensuring hydrogen remains stable, while the energy required for compression and storage. These parameters and their importance are further examined later.
- **Environmental and Safety Factors:** To mitigate environmental risks, the storage site must avoid contamination of nearby freshwater aquifers and minimize potential hazards to surrounding areas. Additionally, locating storage sites away from densely populated regions is crucial for safety.

By fulfilling these criteria, a geological formation can provide an efficient, secure, and sustainable solution for underground hydrogen storage. These factors are pivotal to advancing hydrogen's role as a cornerstone of the global transition to a renewable energy economy. [3][9]

2. Underground Storage Types

2.1. Salt Caverns

Salt caverns are among the most reliable and efficient geological formations used for underground hydrogen storage (UHS). These artificial cavities are created through a process called solution mining, where water is injected into underground salt deposits to dissolve the salt. The resulting hollow chamber is then used to store hydrogen under high pressure. Salt caverns are particularly suitable for hydrogen storage due to their unique structural and chemical properties.

One of the primary advantages of salt caverns is their natural impermeability. Salt formations have an extremely low permeability, which prevents hydrogen from escaping through

the cavern walls. This impermeable nature ensures a high level of containment, making salt caverns one of the safest options for large-scale hydrogen storage. Additionally, the plasticity of salt allows it to self-seal any minor cracks or fractures, further enhancing its ability to securely store hydrogen over long periods.

Salt caverns are also structurally robust, capable of withstanding the high pressures required for hydrogen storage, which is crucial for maintaining the integrity of the storage site, even under the cyclic stresses associated with frequent injection and withdrawal of hydrogen. Despite their many advantages, salt caverns are not widely accessible around many parts of the world and their storage capacity is smaller compared to other geological formations such as depleted reservoirs or aquifers. [10]

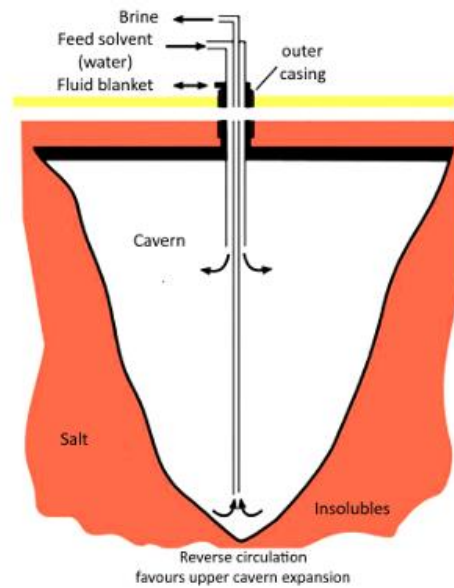


Figure 2 Salt Cavern [53]

2.2. Depleted Gas and Oil Reservoirs

Depleted oil and gas reservoirs are highly promising options for underground hydrogen storage due to their large capacity and existing infrastructure. These porous rock formations found at optimal depths of up to 2,000 meters [5] which previously held hydrocarbons offer proven

containment over geological timescales, making them ideal for long-term, large-scale hydrogen storage. Their extensive pore volumes allow for significant seasonal storage, enabling hydrogen to be stored during periods of low demand and retrieved during peak demand, supporting renewable energy integration.

One of the many advantages of these reservoirs is the presence of pre-existing infrastructure, such as wells and pipelines, which can be adapted for hydrogen storage. This reduces the cost and time required for development. However, the integrity of the reservoir and its caprock must be carefully assessed, as hydrogen's small molecular size increases the risk of leakage. Ensuring a robust seal is crucial for safe and reliable storage. Challenges also arise from potential interactions between hydrogen and residual hydrocarbons producing gases such as H_2S and CH_4 with loss of hydrogen, which could lead to contamination or storage inefficiencies. Despite these issues, depleted reservoirs remain a cost-effective and scalable solution for hydrogen storage, especially in regions with abundant renewable energy and a need for large-scale storage. With advanced site assessments and technological developments, these formations can play a significant role in supporting a hydrogen-based energy system. [11]

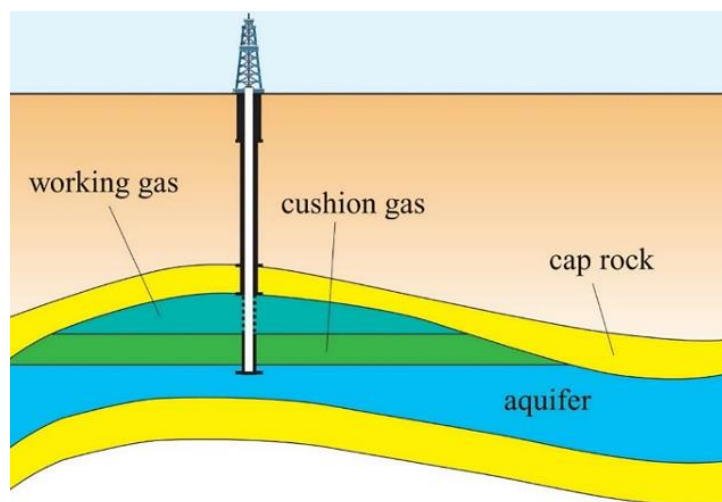


Figure 3 Depleted hydrocarbon reservoir [11]

2.3.Saline Aquifer Formations

Saline aquifers, found in sedimentary basins, offer significant potential for underground hydrogen storage (UHS) due to their global availability and high storage capacity. These formations consist of porous rock filled with high-salinity brine, sealed by impermeable caprock, making them suitable for large-scale and seasonal storage. Hydrogen can be stored during periods of excess energy production and retrieved during peak demand, supporting renewable energy integration. [11]

However, saline aquifers pose challenges, including potential chemical interactions between hydrogen, brine, and reservoir rock, which may result in storage losses. Site-specific assessments, including geophysical surveys and reservoir monitoring, are essential to ensure safety and efficiency. Operational experience with pure hydrogen in saline aquifers remains limited, necessitating further research and technological development. Despite these challenges, saline aquifers represent a scalable and widely available solution for hydrogen storage, particularly in regions lacking other geological options. With advancements in monitoring and storage technology, they can play a crucial role in supporting a hydrogen-based energy system. [12]

3. Trapping Mechanisms

3.1.Structural Trapping

Structural trapping is a vital mechanism for the underground storage of hydrogen, where geological formations prevent the upward migration of hydrogen gas due to buoyancy. This process relies on the presence of a caprock, an impermeable layer that acts as a seal, effectively

containing hydrogen within the subsurface. The caprock's high capillary entry pressure is crucial, as it ensures that hydrogen remains trapped despite its tendency to rise.

The effectiveness of structural trapping is influenced by several factors, including the geological characteristics of the reservoir and the thermodynamic conditions present. The interplay between pressure and temperature significantly affects hydrogen density and its behavior in geological formations. For instance, as pressure increases with depth, the buoyancy forces acting on hydrogen are countered by capillary forces, allowing for stable storage. It should be mentioned that the trapped gas beneath the sealing rock is very mobile, so even with the trapping structures, there is a possibility for leakage to occur. H_2 gas, which is much more mobile than other gases like CO_2 , may raise the pressure within the reservoir during the injection phase, triggering new faults and fractures that would enable the mobile H_2 gas to escape via slow diffusion [13].

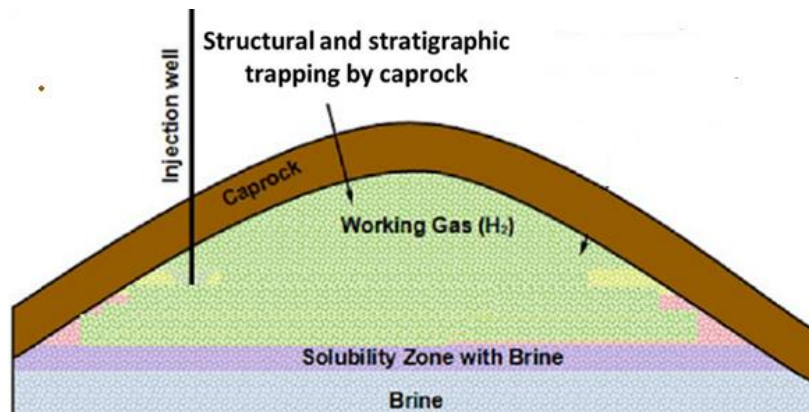


Figure 4 Structural trapping by caprock [13]

3.2. Capillary Trapping

Capillary trapping plays a crucial role in securely immobilizing hydrogen within porous geological formations, contributing to the efficiency and safety of underground hydrogen storage (UHS). This mechanism occurs when hydrogen, as a non-wetting phase, is injected into porous rocks, displacing the wetting fluid (usually brine) from the larger pore spaces. Once injection stops,

capillary forces cause the wetting fluid to re-enter smaller pores, trapping hydrogen as residual gas that remains immobile. This trapping mechanism is vital for UHS, as it minimizes the risk of hydrogen leakage, even in the absence of perfect structural or stratigraphic traps and complements other trapping mechanisms such as structural trapping, providing an added layer of security to large-scale hydrogen storage projects. [10]

3.3.Solubility Trapping

This mechanism works when hydrogen dissolves into the formation water (brine) under high pressure conditions and is dependent on the pH, temperature, salinity and on the pore fluid properties. Additionally, the dependence on solubility trapping is generally unfavorable for hydrogen storage since hydrogen has a low solubility in brine compared to other gases like CO₂. Therefore, it can take thousands of years for the hydrogen to dissolve in brine. So, the possibilities of dissolution trapping are extremely low, mainly when the storage scenario is non-permanent. These factors make solubility trapping a less efficient and less reliable mechanism for short term hydrogen containment. [14][15]

3.4.Mineral Trapping

This process is even slower than solubility trapping and also takes thousands or even millions of years for it to occur, contingent on the rock minerals, gas pressure, temperature and formation porosity. Consequently, mineral trapping is not considered as a primary mechanism for short term hydrogen storage.

After discussing the main trapping mechanisms, it can be concluded that the main trapping phenomena that can be relied on for effective hydrogen storage are structural and capillary trapping, since the dynamic simulation for UHS is done for a span of only 10 years. [16]

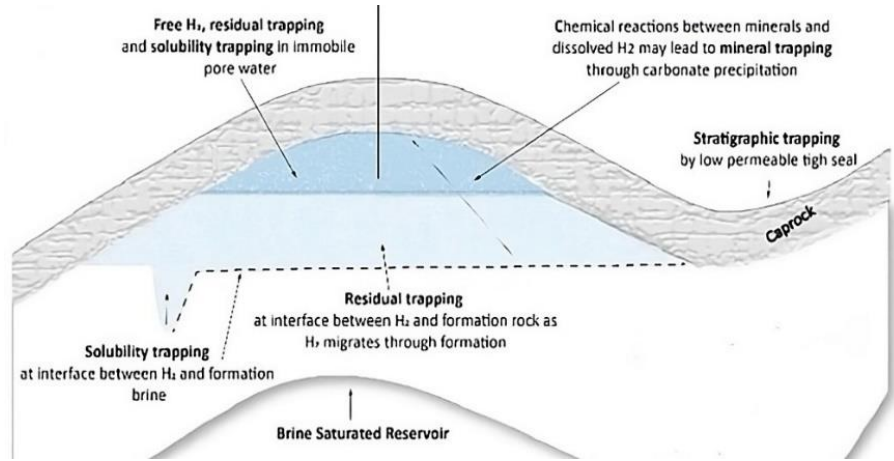


Figure 5 H_2 Trapping mechanisms overview [16]

4. Rock-Fluid Properties

The successful implementation of UHS depends on a comprehensive understanding of the complex interactions between hydrogen and geological formations. These interactions are governed by various rock-fluid properties, which play a crucial role in determining the efficiency of hydrogen injection, storage stability, and extraction from underground reservoirs. [17]

4.1. Interfacial Tension

Interfacial tension is one of the most critical parameters concerned with UHS, as this property determines the interaction of hydrogen with the fluids present in geological formations. Interfacial tension refers to the energy required to create a boundary between two immiscible fluids, such as hydrogen and brine and is an important variable that allows one to assess the efficiency of storage and recovery of hydrogen from underground environments.

Recent research conducted provide valuable insights into the IFT of hydrogen-water systems under varying conditions using the pendant-drop method for IFT measurement at temperatures from 25 °C up to 150 °C and pressures up to 35 MPa as seen in the figure below (Fig.6) [19]. For example, at a constant temperature of 25 °C, the IFT was about 75 mN/m at 1 MPa and decreased to about 72 mN/m at 35 MP. Similarly, at a constant pressure of 1 MPa, the IFT decreased substantially while going from 75 mN/m at 25 °C to 50 mN/m at 150 °C.

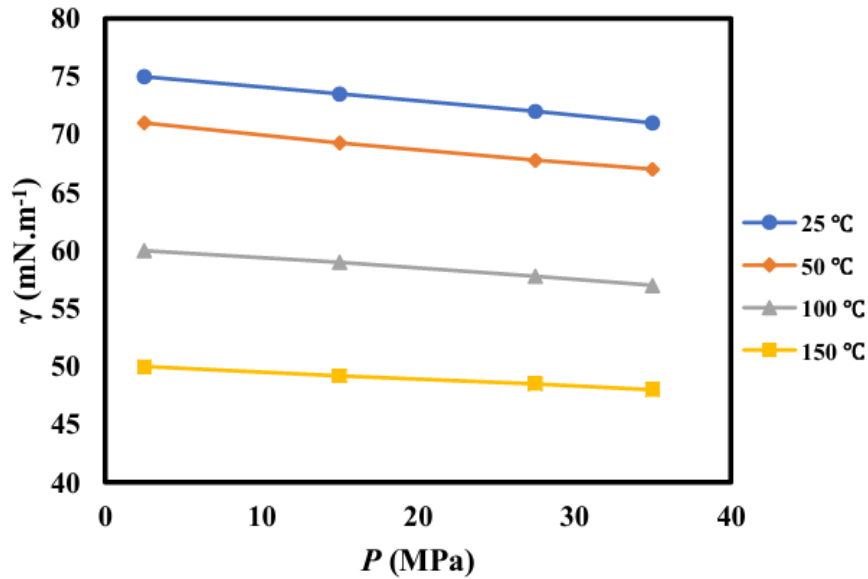


Figure 6 Effect of pressure on the IFT of H₂-brine system [19]

The general trend is that IFT decreases with the increase of pressure and temperature, which enhances the ability of hydrogen to displace other fluids within rock pores. Inversely, higher salinity will lead to a higher value of IFT because of the more intermolecular interactions among ions and water molecules (Fig.7). Hydrogen-IFT rock interaction has important implications as low IFT values enhance the ability of hydrogen to displace resident fluids such as brine or oil from the pore spaces in the rocks, a prerequisite for attaining maximum storage and efficient recoveries upon extraction [19].

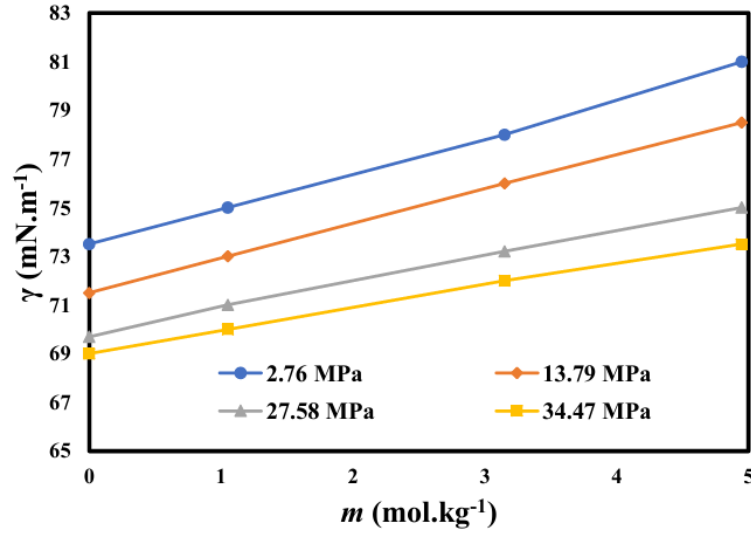


Figure 7 Salinity effect on IFT in H₂-brine system [19]

In addition, high IFT could lead to capillary entrapment, a condition whereby hydrogen is effectively immobilized by surface tension forces within pore spaces. Moreover, with variation in IFT, wettability may be varied concerning changes in how the fluids meet the rock surface since favorable wettability promotes better flow of hydrogen through the reservoir, whereas unfavorable wettability could cause entrapment, hence a drop in efficiency. [20]

4.2. Wettability and Contact Angle

In UHS, wettability influences how hydrogen interacts with geological formations and the fluids present within them. It is quantified by the contact angle, which measures the angle formed at the interface between a solid surface, a liquid, and a gas.

A study conducted by Iglauer et al. (2021) investigated the wettability of sandstone reservoirs under realistic geological conditions. The researchers found that sandstone surfaces exhibited weakly water-wet to intermediate-wet characteristics when exposed to hydrogen. Specifically, they measured contact angles at various pressures and temperatures, revealing that increasing pressure and temperature enhanced hydrogen wettability. For instance, at 25 MPa and 323 K, the advancing

contact angle was recorded at 77° , while the receding contact angle was 71° . These values indicate that hydrogen exhibits a tendency to displace brine in these conditions, which is favorable for storage and withdrawal applications [21]. The study also demonstrated that the presence of organic molecules on sandstone surfaces significantly also affects wettability. For instance, when quartz substrates were aged with stearic acid to simulate organic contamination, the contact angles increased, indicating enhanced hydrophobicity. As seen in the graph below (Fig.9), at a stearic acid concentration of 10^{-2} mol/L and the same pressure and temperature conditions mentioned earlier, the advancing contact angle increased to 77° compared to lower values observed on pure uncontaminated quartz surfaces.

The influence of pressure on contact angle was particularly pronounced in this study, as pressure increased from 0.1 MPa to 25 MPa, θ_a rose from 0° to 49° at 343 K, demonstrating that higher pressures enhance hydrogen wettability. Similarly, temperature increases also correlated with higher contact angles since at 10 MPa, θ_a increased from 12.5° at 296 K to 34° at 343 K, as shown in the graph below (Fig.8). Therefore, higher temperatures and pressures lead to higher contact angles between H_2 and the rock surface, generally facilitating better displacement of brine by hydrogen within rock pores, ensuring efficient hydrogen recovery during extraction processes. Conversely, lower contact angles between H_2 and the rock surface can lead to capillary trapping of hydrogen where the gas becomes immobilized, reducing withdrawal efficiency. [22]

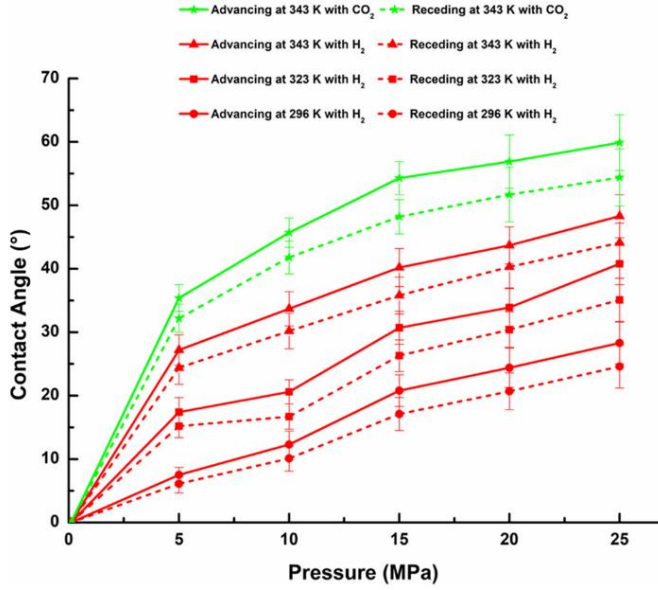


Figure 8 Brine contact angles on the pure quartz surface in H_2 -atmosphere as a function of Pressure and Temperature [21]

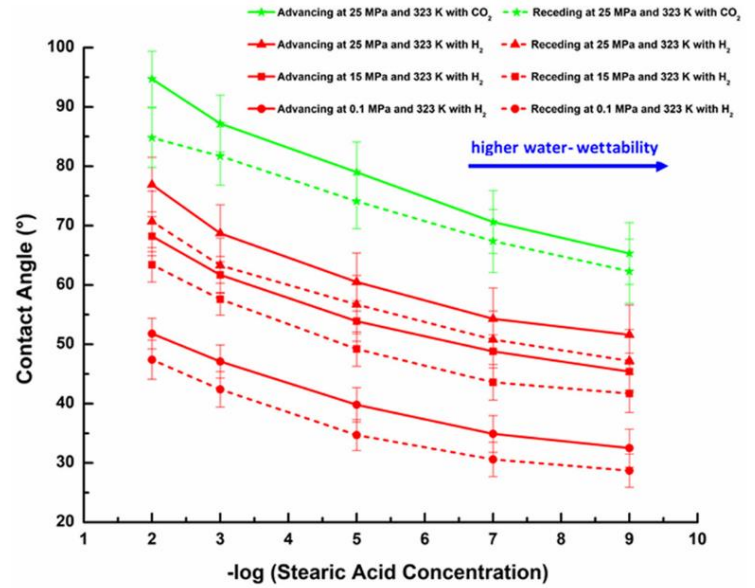


Figure 9 Brine contact angles on the quartz surface in the H_2 -atmosphere as a function of stearic acid concentration [21]

4.3. Capillary Pressure

The impact of capillary pressure on UHS is primarily observed through hysteresis phenomena in capillary pressure - saturation relationships (Fig.10). While the inclusion of capillary pressure scanning curves may not considerably impact bulk storage efficiency, it significantly affects properties such as withdrawal rates and pressure dynamics. Capillary trapping can lead to substantial hydrogen losses during withdrawal cycles as this phenomenon is particularly pronounced at higher pressures and depths, where capillary forces become more dominant. The competition between gravitational, capillary, and viscous forces determines the optimal operational parameters for injection and withdrawal rate. Additionally, the caprocks' ability to prevent hydrogen leakage is influenced by the capillary entry pressure, which is a crucial factor in determining their sealing efficiency for geologically stored gases like hydrogen. [23]

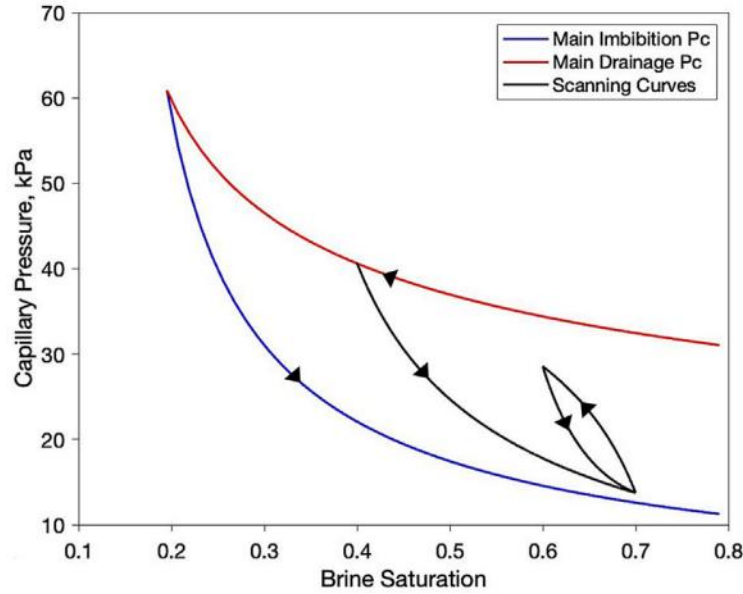


Figure 10 Capillary pressure hysteresis curves [23]

4.4. Relative Permeability Hysteresis

Relative permeability critically influences UHS efficiency by governing fluid flow dynamics in porous media, it describes how easily hydrogen can flow through porous media in the presence of other fluids such as water or oil. Since Hydrogen undergoes cyclic injection and withdrawal periods multiple times a year, variations in relative permeability between cycles occur due to hysteresis, where flow pathways do not return to their original state after each cycle, as can be seen in (Fig.11). To accurately model these hysteresis effects, various mathematical models have been developed, and among them is Killough's hysteresis model, introduced in 1976, has gained prominence for its ability to simulate hysteresis in both wetting and non-wetting phases. This model generates smooth scanning curves between drainage and imbibition processes, enhancing the prediction of fluid behavior during cyclic saturation changes. [24]

Killough's model has been widely adopted in reservoir simulations, especially for processes like water-alternating-gas (WAG) injection, where cyclic saturation changes are prevalent. By

incorporating hysteresis effects, this model improves the accuracy of simulations, leading to better predictions of reservoir performance.

Moreover, Lysyy et al. (2022) demonstrated significant hysteresis effects in hydrogen-water relative permeability during drainage and imbibition cycles, highlighting complex rock-fluid interactions that impact storage performance. Pore-scale modeling has shown that relative permeability variations can substantially affect hydrogen trapping mechanisms and the relationship between capillary, viscous, and gravitational forces creates non-linear flow behaviors that significantly impact injection and withdrawal efficiency [24]. These interactions determine the ultimate recoverable hydrogen volume and storage system performance. Moreover, Nazari et al. (2024) emphasized that neglecting relative permeability hysteresis in numerical models can lead to substantial overestimations of recoverable hydrogen. [23]

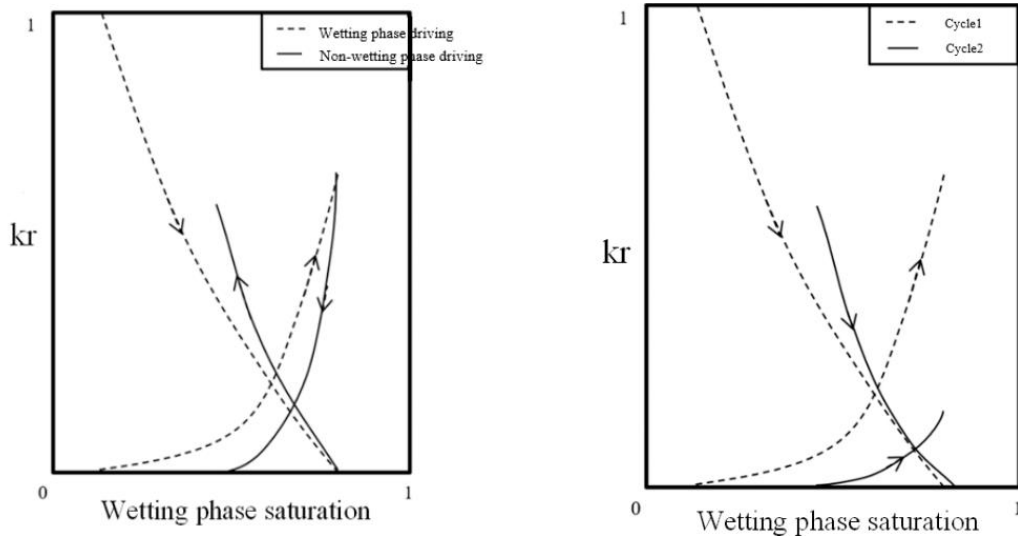


Figure 11 Relative permeability hysteresis curves: Displacement direction dependent (left), Saturation history dependent (right) [53]

5. Diffusivity

Hydrogen diffusivity describes the ability of hydrogen molecules to move through a geological medium. Based on thorough research, diffusivity is influenced by multiple factors such as temperature, pressure, brine salinity, and the properties of the transport medium. In addition, hydrogen's small molecular size makes it more mobile than other gases and particularly susceptible to potential leakage through caprocks. The significance of hydrogen diffusivity lies in its role in determining potential hydrogen loss during storage. Hydrogen has a relatively high diffusion rate in water or brine compared to other gases, which makes understanding its migration characteristics crucial. [25].

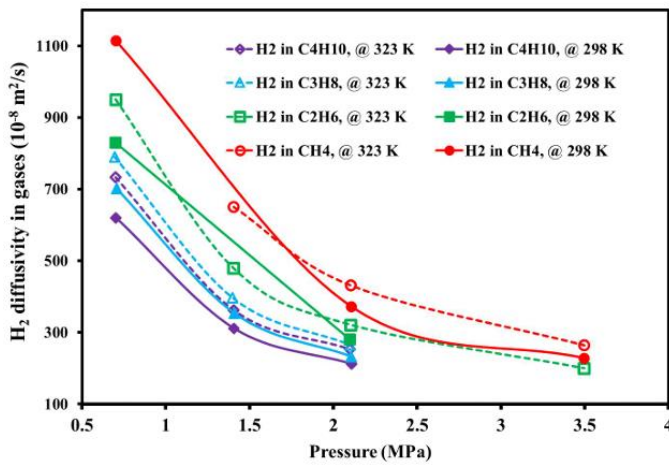


Figure 12 H_2 diffusivity for hydrocarbon fluids as a function of temperature and pressure [26]

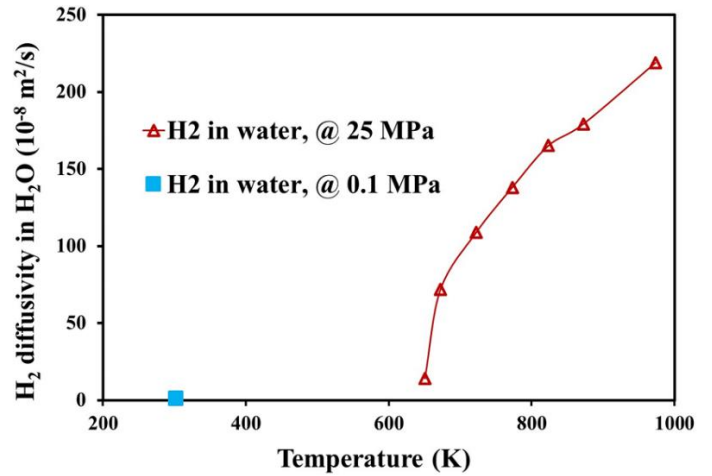


Figure 13 H_2 diffusivity in brine as a function of temperature and pressure [26]

Plot observations reveal that the temperature and pressure significantly impact hydrogen diffusivity. At higher temperatures and pressures, hydrogen diffusion behavior can change dramatically, it can be seen from (Fig.12) that the hydrogen diffusivity in hydrocarbon fluids followed a decreasing trend with increasing temperature and pressure [26]. When the pressure increased from 0.6 MPa to 3.5 MPa, at a constant temperature of 323 K, hydrogen diffusivity rate

in C_2H_6 decreases from $950 \times 10^{-8} \text{ m}^2/\text{s}$ to $260 \times 10^{-8} \text{ m}^2/\text{s}$. Whereas in water, hydrogen diffusivity rate increased from $16 \times 10^{-8} \text{ m}^2/\text{s}$ at 650 K to $220 \times 10^{-8} \text{ m}^2/\text{s}$ at a temperature and pressure of 970 K and 25 MPa respectively, as shown in the graph (Fig.13). When comparing both cases (Fig.9 and Fig.10), it is evident that hydrogen has a relatively higher diffusion rate in brine compared to hydrocarbon gases. In addition, salinity also plays a critical role, with studies showing that hydrogen self-diffusivities decrease linearly with increasing salinity [27].

6. Potential Risks

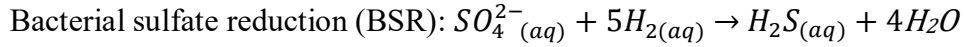
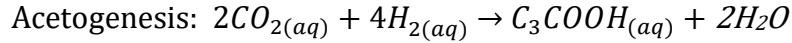
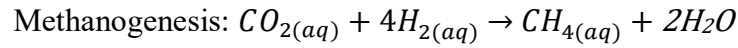
Underground hydrogen storage (UHS) faces several challenges that impact its safety and efficiency. Microbial activity, particularly from methanogens and sulfate-reducing bacteria, can consume hydrogen and produce methane (CH_4) and hydrogen sulfide (H_2S), altering gas composition. Geochemical reactions with reservoir rocks may also affect storage conditions by changing porosity and permeability. Additionally, cyclic hydrogen injections and withdrawal create mechanical stress, potentially compromising caprock integrity and increasing leakage risks. Due to hydrogen's small molecular size and high diffusivity, ensuring long-term containment is crucial. Addressing these risks through proper site selection and monitoring is essential for effective hydrogen storage. [28]

6.1. Microbial Reactions

Recent research has shed light on the significant influence of microbial activities on the long-term stability of underground hydrogen storage systems. Microorganisms, particularly methanogens, acetogens, sulfate-reducing bacteria (SRB), and iron-reducing bacteria (IRB), can consume stored hydrogen, potentially leading to losses of up to 12% over several months [29]. This consumption not only reduces hydrogen availability but also produces various byproducts

that pose risks and affect storage stability and results in potential loss of stored hydrogen due to microbial consumption.

Acetogen bacteria could produce acetic acid when reacting with H₂ and CO₂, while methanogens, for instance, can convert H₂ and CO₂ into CH₄, leading to a decrease in hydrogen content and altering the gas composition, while Bacterial sulfate reduction (BSR) produce hydrogen sulfide (H₂S), a corrosive and toxic gas that compromises storage safety:



This process was observed in the Lobodice town gas storage facility in the Czech Republic, where a 17% decrease in hydrogen was accompanied by a concurrent decrease in CO₂ and an increase in CH₄ of 18% over a seven-month cycle. Moreover, Laboratory studies have shown hydrogen consumption rates ranging from 0.008 to 5.8×10⁻⁵ nM/hr for methanogens, and 0.005 to 130 × 10⁵ nM/hr for sulfate reducers (SRBs) [30] [31]. Therefore, the rate of hydrogen consumption by microbes can vary significantly depending on environmental conditions. However, it's important to note that these rates may not directly translate to field conditions due to various factors such as temperature, pressure, and nutrient availability.

In addition, microbial hydrogen consumption can lead to significant pH increases up to a value of 9 in some cases, affecting microbial activity and mineral dissolution/precipitation processes. These activities can induce the precipitation of minerals like siderite (FeCO₃) or pyrite (FeS₂), altering reservoir properties and affecting hydrogen retention [29][32]. The impact of microbial

activity varies between reservoir types, for example, SRBs, IRBs, and halophilic methanogens dominate in saline aquifers, while depleted reservoirs support more diverse populations including hydrocarbon-degrading bacteria. Different microbial groups engage in complex interactions, creating a dynamic ecosystem that can impact storage stability over time.

In fact, recent studies have also highlighted the potential for microbial activity to alter the wettability of the hydrogen/brine/rock system, which can impact flow dynamics and trapping mechanisms in the reservoir. This underscores the complexity of microbial interactions in UHS and the need for comprehensive research to fully understand and mitigate potential risks [33][34].

6.2. Geochemical Reactions

Storing hydrogen underground (UHS) in depleted hydrocarbon reservoirs poses several geochemical challenges that could impact both efficiency and safety. Recent studies have provided new insights into these risks, confirming some previous concerns while dispelling others.

One of the main issue is the potential loss of hydrogen due to geochemical interactions with reservoir rocks and fluids. However, a comprehensive study by Hassanpouryouzband et al. (2022), which involved over 250 batch reaction experiments on various sandstone reservoirs under subsurface conditions, found that abiotic geochemical reactions posed no considerable risk of hydrogen reduction or decline of reservoir integrity. This finding mitigates initial concerns regarding the geochemical stability of sandstone reservoirs for hydrogen storage [35]. Despite this, hydrogen sulfide (H_2S) formation remains a critical issue since reactions between hydrogen and sulfur-bearing minerals such as pyrite, can generate H_2S which is a toxic and corrosive gas. According to Homoud et al. (2025), H_2S concentrations could reach 13 ppm in certain conditions, making desulfurization necessary to ensure storage safety and performance since the presence of

H₂S could compromise infrastructure integrity and pose safety hazards [36]. Moreover, mineral dissolution and precipitation reactions are another potential concern, though their effects may be less severe than initially expected as these reactions could alter the reservoir's porosity and permeability, potentially influencing storage capacity and injectivity.

In addition, injecting hydrogen can also modify the chemical composition of formation waters, potentially leading to further reactions. Saeed et al. (2023) observed that increasing reservoir pressure from 100 atm to 500 atm resulted in higher levels of dissolved H₂ and CO₂. These changes in brine chemistry could trigger additional geochemical interactions, though their exact impact on storage efficiency is still under investigation. [37]

6.3. Physical Risks

The repeated injection and extraction of hydrogen can cause fluctuations in pressure and stress within the storage reservoir, which may compromise the stability of wells, caprocks, and adjacent rock formations. Such variations in stress can also trigger seismic activity, particularly in regions where faults already exist or where geological stress is prevalent. A primary geo-mechanical hazard in UHS operations is the reactivation of faults. Alterations in the fault's stress state, including changes in normal and shear stress, can influence stress-sensitive fluid flow and increase the possibility of fault movement. The rise in pore pressure due to hydrogen injection may provoke fault slippage, especially when the fault displacement is considerable in relation to the thickness of the reservoir. [38]

The cyclic nature of hydrogen storage can also weaken the mechanical integrity of both the reservoir rock and caprock. The repeated application of stress can lead to the gradual formation of microfractures and modifications in the rock's mechanical behavior over time, potentially

impairing the caprock's ability to retain hydrogen. As a result, the likelihood of gas leakage could rise, threatening the long-term stability of the storage formation. Another geomechanical issue in UHS is ground movement, including both land subsidence and uplift. The continuous injection and withdrawal of hydrogen in significant quantities can alter stress conditions within the reservoir and its surrounding formations, potentially leading to deformations on the surface. [39]

6.4. Caprock Integrity

Caprock integrity is crucial for the safety and efficiency of underground hydrogen storage systems as recent research has provided valuable insights into the potential risks and challenges associated with caprock integrity during UHS operations. Smaller pores, and higher breakthrough pressures significantly enhance the caprock's ability to contain hydrogen, and it is crucial to maintain pressure surges below the capillary entry pressures and fracture initiation pressures of caprocks and fault rocks to ensure storage site integrity [40].

Geochemical interactions between hydrogen, brine, and caprock minerals appear to have minimal impact on caprock integrity. A study by Zeng et al. (2022) suggests that H₂-brine-shale geochemical interactions may not compromise caprock integrity during UHS. Their kinetic batch models showed that the dissolution degrees of all tested minerals in several shale types were less than 1% over 30 years, indicating strong caprock integrity and containment ability from a geochemical perspective (Fig.14). [40]

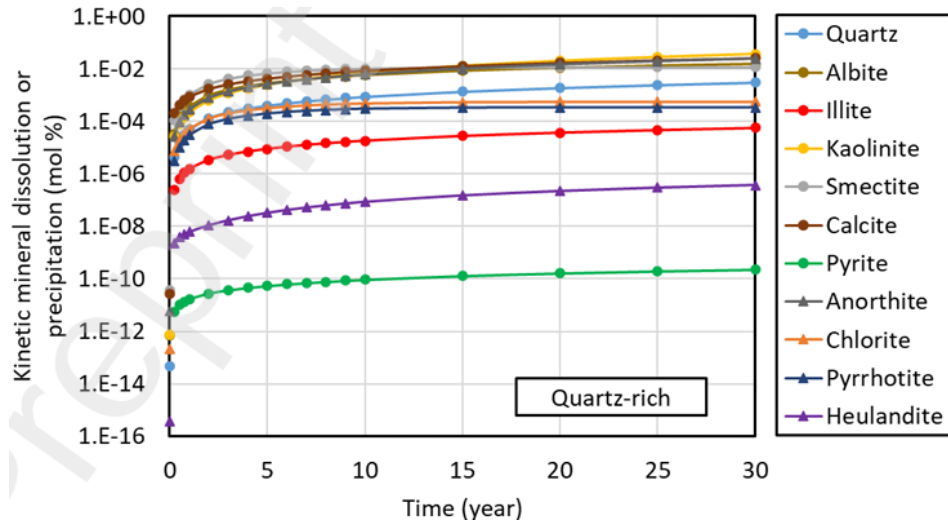


Figure 14 Kinetic dissolution of individual mineral phase of quartz-rich caprock [40]

Caprock thickness is also an important factor in reducing gas leakage rates. The same study found that thicker caprock layers significantly reduce the rate of gas leakage, with CO_2 exhibiting higher mass leakage rates due to its larger molar mass and lower interfacial tension compared to H_2 . However, there are potential risks to caprock integrity during UHS operations because mechanical weakening can occur due to cyclic injection and withdrawal of hydrogen, leading to pressure and stress changes within the caprock, potentially causing micro fractures and changes in mechanical properties over time. [41].

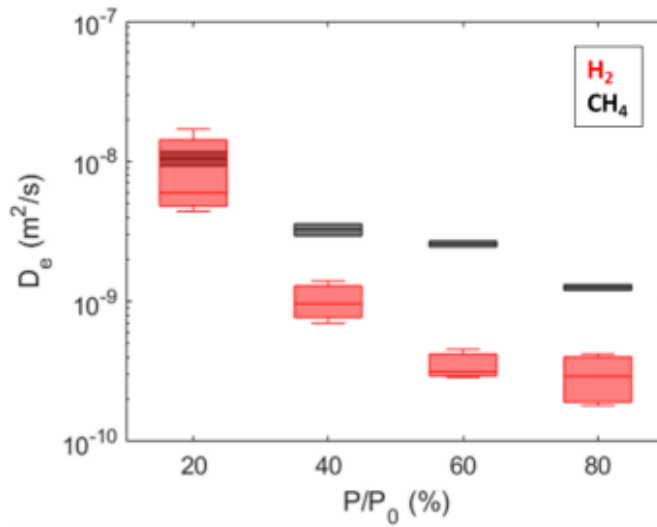


Figure 15 Diffusion coefficient comparison computed for H_2 and CH_4 from wet caprock [42]

Moreover, diffusion is another concern, as recent experimental studies done by Borello et al. (2024), have shown that hydrogen diffusion coefficients in caprocks range from 10^{-10} m²/s to 6×10^{-8} m/s, which is higher than methane (Fig.15). Consequently, this higher diffusivity could lead to caprock increased leakage risks over time. [42]

7. Underground Hydrogen Behavior

Understanding hydrogen's chemical and thermodynamic conditions is essential for accurately predicting hydrogen flow and storage within porous media, which is crucial for the development of safe and efficient large-scale underground hydrogen storage systems. The unique properties of hydrogen, such as its low density and high mobility, present both opportunities and challenges for underground storage. Since the Norne field reservoir is located at a depth of 2500–2700 meters with initial temperatures and pressures of around 90°C and 270 bars respectively, the stored hydrogen is in a supercritical gaseous state during injection and behaves as a highly compressible fluid with gas-like diffusivity and liquid-like density, since it's stored pressure and temperature are significantly higher than its critical temperature and pressure of -240 °C and 1.3 MPa respectively. [43]

Table 2 H₂ Supercritical State Conditions 43]

<i>H₂ Supercritical State Conditions</i>	Values
<i>Temperature</i>	-240 °C
<i>Pressure</i>	1.3 MPa
<i>Density</i>	31 Kg/m ³

The relationship between temperature and pressure in deeper reservoirs significantly impacts hydrogen's density and viscosity, shaping the efficiency and dynamics of underground storage. As depth increases, both pressure and temperature naturally rise due to the weight of overlying geological layers and the geothermal gradient. Hydrogen's density increases with pressure, which is directly proportional to reservoir depth. As shown in the figure below (Fig.16), at shallow depths with low pressures, hydrogen has a low density of around 10 kg/m³, while at depths where pressures reach 50 MPa, its density increases to approximately 40 kg/m³. This increase in density with depth enhances storage efficiency, as hydrogen becomes more compact, allowing a greater amount to be stored within a given volume. However, deeper reservoirs are also subject to higher temperatures, which inversely affect hydrogen's density. For instance, at the same high pressure, hydrogen stored at 40°C is denser than at 120°C. Therefore, deeper reservoirs with higher geothermal gradients may experience a reduction in density compared to cooler formations, potentially offsetting some of the efficiency gains from higher pressures.[44][45]

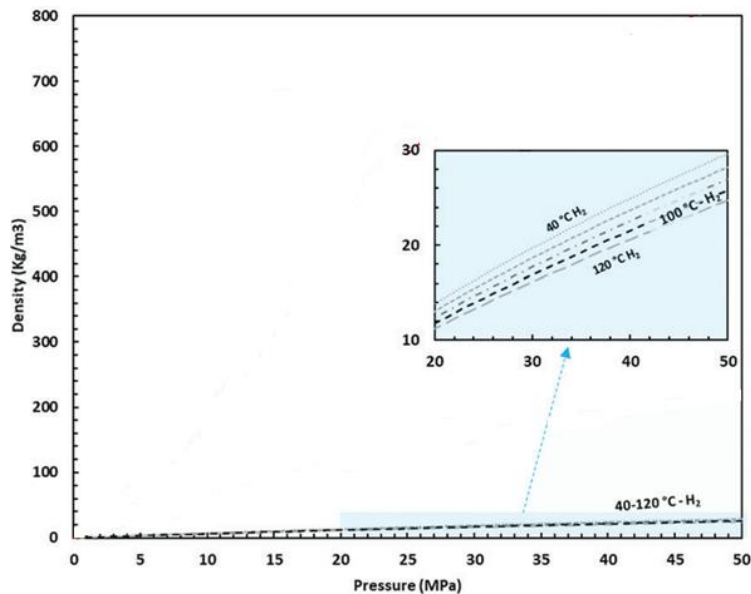


Figure 16 H₂ density in function of Pressure and Temperature [45]

Moreover, storing hydrogen in shallower reservoirs with low hydrogen density relative to the surrounding fluids creates strong buoyancy forces, which become more pronounced as the density

difference increases, driving hydrogen upward within the reservoir. This movement helps hydrogen accumulate beneath impermeable caprocks, simplifying its concentration and retrieval. However, high buoyancy also poses challenges, such as the risk of leakage through fractures or faults in the caprock and lateral spreading in unevenly structured reservoirs. [45]

In contrast, hydrogen's viscosity remains low and relatively unaffected by pressure and temperature variations within the range of typical underground storage conditions ($T < 150\text{ }^{\circ}\text{C}$ and $P < 50\text{ MPa}$). Within the studied range of up to 50 MPa and temperatures from 40°C to 120°C , its viscosity ranges from 9 to $12\text{ }\mu\text{Pa}\cdot\text{s}$ (Fig.17). This low and stable viscosity facilitates hydrogen's movement through porous media, enabling efficient injection and withdrawal during storage operations.[38] [45] However, the high mobility resulting from hydrogen's low viscosity also presents challenges. In reservoirs where pressure gradients are uneven or where geological heterogeneities exist, hydrogen can flow preferentially along high-permeability pathways, leaving portions of the reservoir poorly swept. This phenomenon, known as viscous fingering, can result in trapped hydrogen that is difficult or impossible to recover. Additionally, hydrogen's low viscosity reduces its effectiveness in displacing other in-situ fluids, such as brine, during injection. As a result, some areas of the reservoir may remain saturated with brine, further limiting storage efficiency. [46]

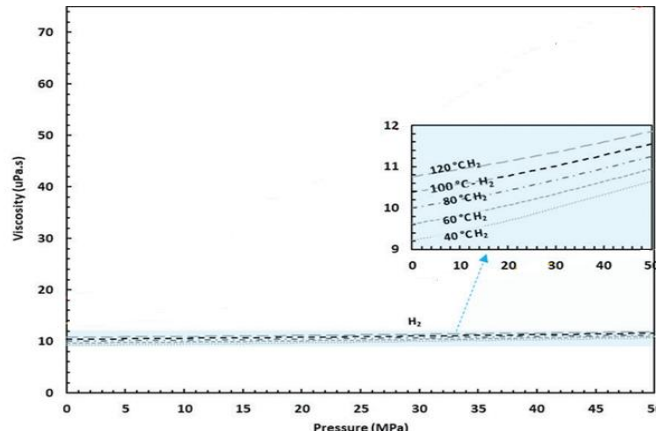


Figure 17 H_2 viscosity in function of Pressure and Temperature [46]

8. Case Studies

➤ **The Rough Gas Field Redevelopment for Hydrogen Storage**

The Rough Gas Field, situated in the UK Continental Shelf, has a long history of gas production since its discovery in 1968. Initially developed for natural gas extraction, it was later converted into a gas storage facility in 1985 and remained in operation until 2017. Following geopolitical and energy supply concerns in 2022, a feasibility study was initiated to assess the potential of repurposing the Rough facility for underground hydrogen storage (UHS). The study was conducted in two phases: the first focused on assessing high-level risks and uncertainties related to hydrogen storage, while the second involved an extensive redevelopment strategy. A new reservoir model was developed, integrating static, dynamic, geomechanical, and thermal analyses to evaluate storage feasibility [47]. The results indicated that the Rough field possesses suitable geological and structural conditions for large-scale hydrogen storage. However, dynamic modeling revealed significant challenges, including hydrogen purity concerns due to cushion gas mixing (primarily CO₂), which required multiple injection and withdrawal cycles to achieve acceptable purity levels. The study also highlighted the importance of pressure management, as hydrogen's low density can lead to higher reservoir pressures at the top of the formation, potentially impacting caprock stability.

Ultimately, the research demonstrated that the Rough field could be successfully converted into a hydrogen storage facility, but achieving operational efficiency required overcoming technical challenges associated with gas mixing, well performance, and long-term pressure stability. [47]

➤ UHS Potential in Depleted Gas Reservoirs in Italy

A study from the EU Hystories project assessed the feasibility of underground hydrogen storage (UHS) in Italy's depleted hydrocarbon reservoirs and saline aquifers. Researchers identified 66 potential UHS sites, both onshore and offshore, with an estimated storage capacity of 69.2 TWh in depleted gas fields currently used for natural gas storage. The findings confirmed that these reservoirs offer a viable solution for large-scale hydrogen storage due to their geological stability and existing infrastructure.

However, the study highlighted significant challenges, including hydrogen's high diffusivity, low density, and reactivity with reservoir materials, which could lead to losses via diffusion, microbial consumption, and geochemical interactions. The research emphasized the need for detailed site-specific assessments and pressure management strategies to maintain storage security.

The study concluded that, despite technical challenges, depleted gas reservoirs in Italy could be successfully repurposed for hydrogen storage with appropriate mitigation strategies. Effective monitoring improved well-sealing technologies, and optimized pressure control measures would be essential to ensuring long-term storage stability. If these factors are addressed, repurposing depleted reservoirs for UHS could significantly contribute to Italy's hydrogen infrastructure, supporting the country's transition to a sustainable energy system. [48]

III. Model Characterization

1. Numerical Simulation and Modeling

To assess the feasibility and performance of underground hydrogen storage, numerical simulation and modeling play a crucial role in predicting reservoir behavior under varying operational conditions. This chapter focuses on the investigation of the static model and geological properties of the reservoir, in addition to the development of dynamic reservoir models in order to analyze different forecast scenarios for Hydrogen storage in a depleted hydrocarbon reservoir. The Norne field has been selected as the case study for this simulation, providing a well-characterized geological formation for evaluating hydrogen storage dynamics. Moreover, The Norne field model grid and reservoir data used in this study were obtained from the Open Porous Media (OPM) website, an open-source platform that provides publicly available reservoir datasets for research and development purposes. [56]

The static model, visualized using Petrel, will define the reservoir's structural framework, lithology, and petrophysical properties, ensuring an accurate representation of the geological conditions affecting hydrogen storage and migration. Then, the historical reservoir production and pressure profiles will be presented before moving on to the dynamic model that is developed on ECLIPSE 100 and will simulate the behavior of hydrogen during multiple injection / withdrawal cycles throughout 3 cases, with the results visualized on Petrel and Eclipse Office.

2. Static Model and Geological Description

The Norne field is an oil and gas field discovered in 1991, it is situated within Blocks 6008/10 and 6508/10 on a horst block located in the southern region of the Nodland II area in the Norwegian Sea (Fig.18). It consists of five heavily faulted formation layers: Garn, Not, Ile, Tofte and Tilje.



Figure 18 map representing the Norne field location

The reservoir, located at a depth of 2578–2700 meters, has a total thickness of 224 meters, with hydrocarbon-bearing formations primarily composed of fine-grained sandstones deposited from the Late Triassic to Middle Jurassic periods. These geological characteristics make it a promising candidate for underground hydrogen storage due to its favorable porosity, permeability, and natural sealing mechanisms. The average porosity ranges from 25%, ensuring sufficient pore space for hydrogen injection and retention, while the permeability varies between 20 and 2500 mD,

suggesting that fluid movement within the reservoir can be effectively controlled, allowing for stable injection and withdrawal rates. The presence of a caprock provides a natural seal, minimizing the risk of hydrogen leakage and ensuring long-term containment.

Structurally, the gas cap is located at the top of the “Garn” Formation, where gas was primarily accumulated, with an average thickness of 31 meters, porosity of 24% and a permeability of 800 mD, making this region particularly suitable for hydrogen injection, as it was already acting as a natural gas storage zone during hydrocarbon production. the “Ile” and “Tofte” formations, containing oil, are situated Below the Gas cap’s “Garn” Formation, and are separated from the gas-bearing layer by the impermeable “Not” Formation. This stacked sealing system enhances the overall security of hydrogen storage, reducing the likelihood of vertical gas migration and maintaining reservoir integrity even under repeated injection and withdrawal cycles.

Additionally, the previous presence of hydrocarbons indicates that the reservoir has maintained gas for geological timescales, further confirming its suitability for long-term hydrogen storage applications. The static model was done on petrel and consists of 113344 grid cells of which 44927 are active (Fig.19).

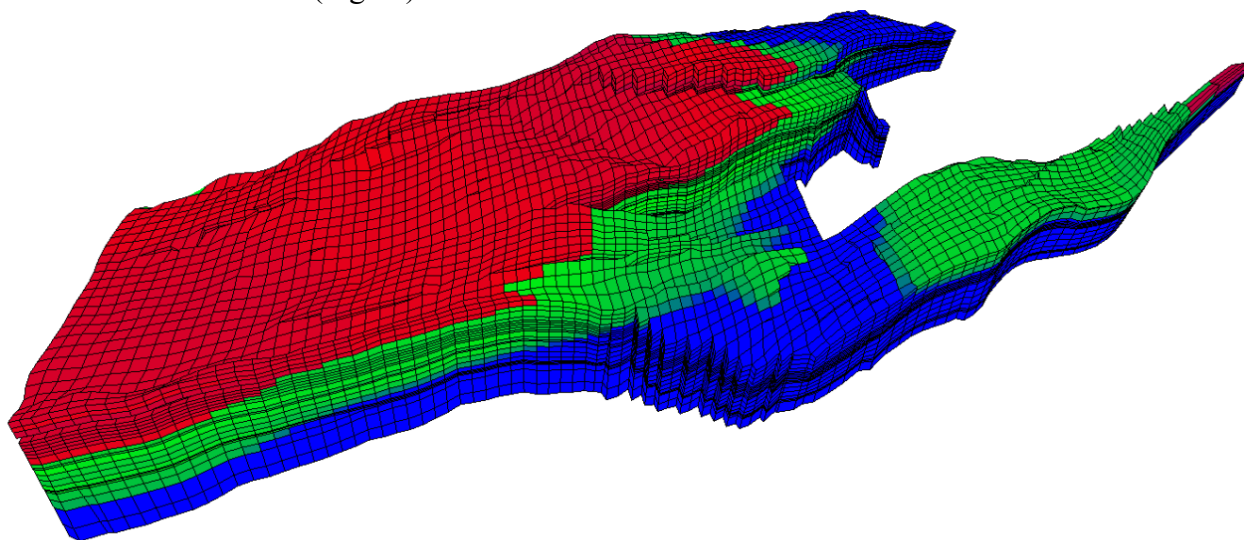


Figure 19 3D view of the grid

The prospective properties of the gas cap and overall reservoir properties mentioned above are reported in the tables below.

Table 3 Reservoir properties

Properties	Reservoir	Gas Cap
<i>Total number of wells</i>	36 wells	8 wells
<i>depth</i>	2578-2802 m	2578
<i>Initial Pressure</i>	170 bars	170 bars
<i>Total thickness</i>	224 m	31 m
<i>Average Porosity</i>	~25 %	~24 %
<i>Average Permeability</i>	20-2500 mD	~800 mD
<i>Average Sw_i</i>	~0.19	~ 0.15
<i>Net-to-Gross</i>	0.7-1	~1

3. Dynamic model

The dynamic simulation of underground hydrogen storage in the Norne field was conducted using ECLIPSE 100 and visualized on Petrel and Eclipse office, where a mixture of natural gas alongside hydrogen is injected for all the three forecast scenarios tested. The dynamic simulation of hydrogen storage in the Norne field was conducted using the ECLIPSE 100 simulator, as the publicly available Norne model was originally developed in this framework. Given the limitations of the black oil model, the Solvent option in ECLIPSE 100 was employed to introduce hydrogen as a distinct dry gas phase. Its properties were derived from literature sources to ensure an accurate representation of hydrogen behavior within the reservoir [55]. This approach enabled differentiation between both the injected natural gas and hydrogen. Thus, by applying the Solvent

function, the injected gas was modeled with a hydrogen fraction of 0.3 and a natural gas (methane) fraction of 0.7, effectively representing the injection strategy while maintaining compatibility with the existing Norne dataset. While this approach enabled an approximation of hydrogen storage dynamics, it does not fully account for the detailed thermodynamic interactions and phase behavior of hydrogen, which would require a compositional simulation approach for a more precise evaluation of subsurface storage performance.

Since the Norne field is originally a depleted hydrocarbon reservoir with an established production history, the study focused on repurposing its existing wells within the gas cap region as injection and production points, ensuring a realistic assessment of UHS feasibility while minimizing the need for new infrastructure. The objective was to evaluate how different injection and withdrawal strategies influenced storage efficiency, pressure stability, and recovery potential while ensuring that reservoir conditions remain within safe operational limits. As previously discussed, given the cyclic nature of hydrogen injection and withdrawal, hysteresis effects were explicitly accounted for using Killough's hysteresis model for both the wetting and non-wetting phases, as this approach enables a more realistic prediction of gas trapping, residual hydrogen saturation, and mobility shifts occurring during cyclic storage operations [24]. Thus, three cases with different rates and well configurations were evaluated in the same timeframe with the same constraints. A maximum BHP constraint of 270 bars was imposed, corresponding to the initial gas cap regional pressure, preventing excessive stress that could lead to fractures or leakage risks. Likewise, a minimum BHP constraint of 130 bars was set to maintain sufficient pressure support for gas withdrawal and to prevent excessive reservoir depletion that could reduce production efficiency. Moreover, the simulations were structured to evaluate hydrogen retention and production performance over a total period of 10 years from 2019 until 2029. It consists of an

initial infilling period implemented to stabilize reservoir pressure before cyclic operations began. This was followed by four storage cycles, each consisting of seven months of injection and five months of withdrawal. Finally, a two-year prolonged withdrawal phase was introduced at the end of the cycles, intended to simulate the long-term production feasibility of stored hydrogen. Important indicators included gas in place (GIP), regional pressure evolution, and hydrogen distribution. GIP trends determined the storage efficiency and recoverability of hydrogen, while pressure variations ensured safe operational limits were maintained throughout the injection and withdrawal cycles. The distribution of hydrogen was examined to assess gas mobility, retention losses, and overall storage stability under different well configurations. By comparing the results across all three cases, the study aimed to determine the most efficient storage and production strategy while maintaining reservoir stability and optimizing hydrogen recovery.

3.1. Reservoir Injection, Production and Pressure History

The historical production and pressure trends of the Norne field were reproduced by the 3D model and provided valuable insights into reservoir depletion behavior and the impact of production strategies on pressure variations before evaluating its suitability for underground hydrogen storage. Figures (Fig.21), (Fig.22), and (Fig.23) present the cumulative production of gas, oil and water, while (Fig.20) shows the reservoir pressure decline over time, illustrating the impact of hydrocarbon extraction and enhanced recovery methods on pressure dynamics.

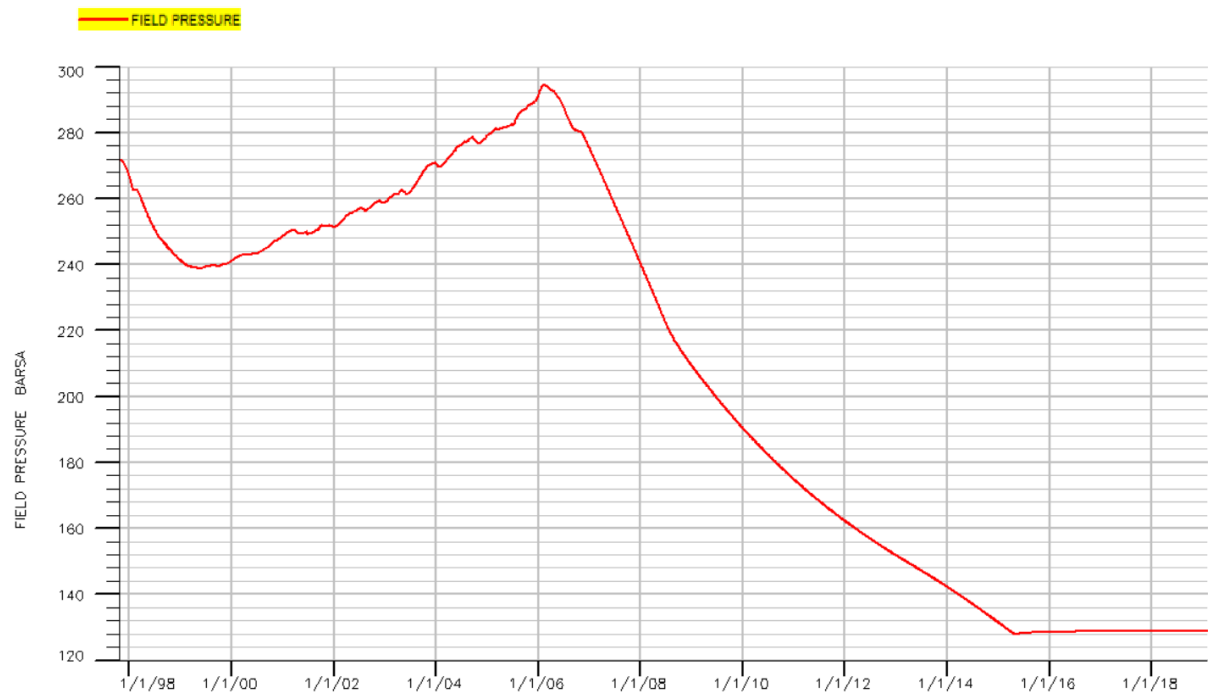


Figure 21 Field Pressure Plot

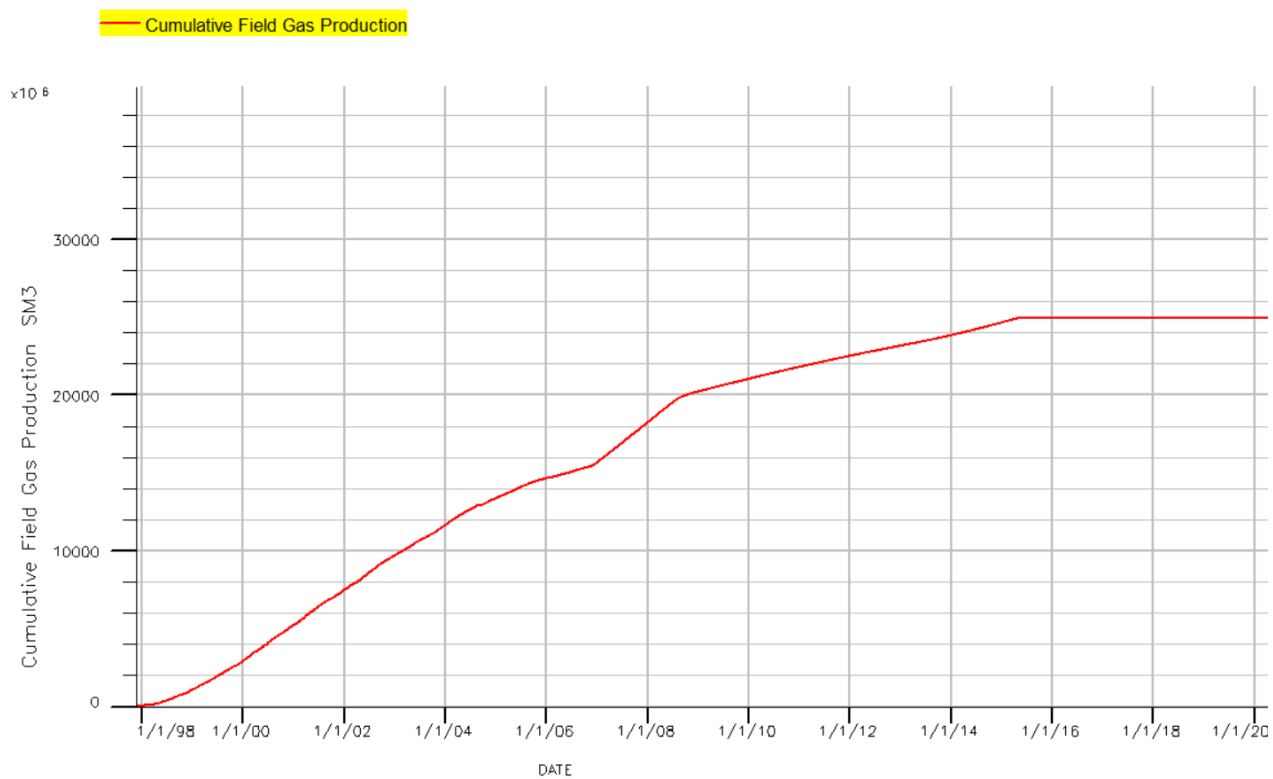


Figure 20 Cumulative Field Gas Production Plot

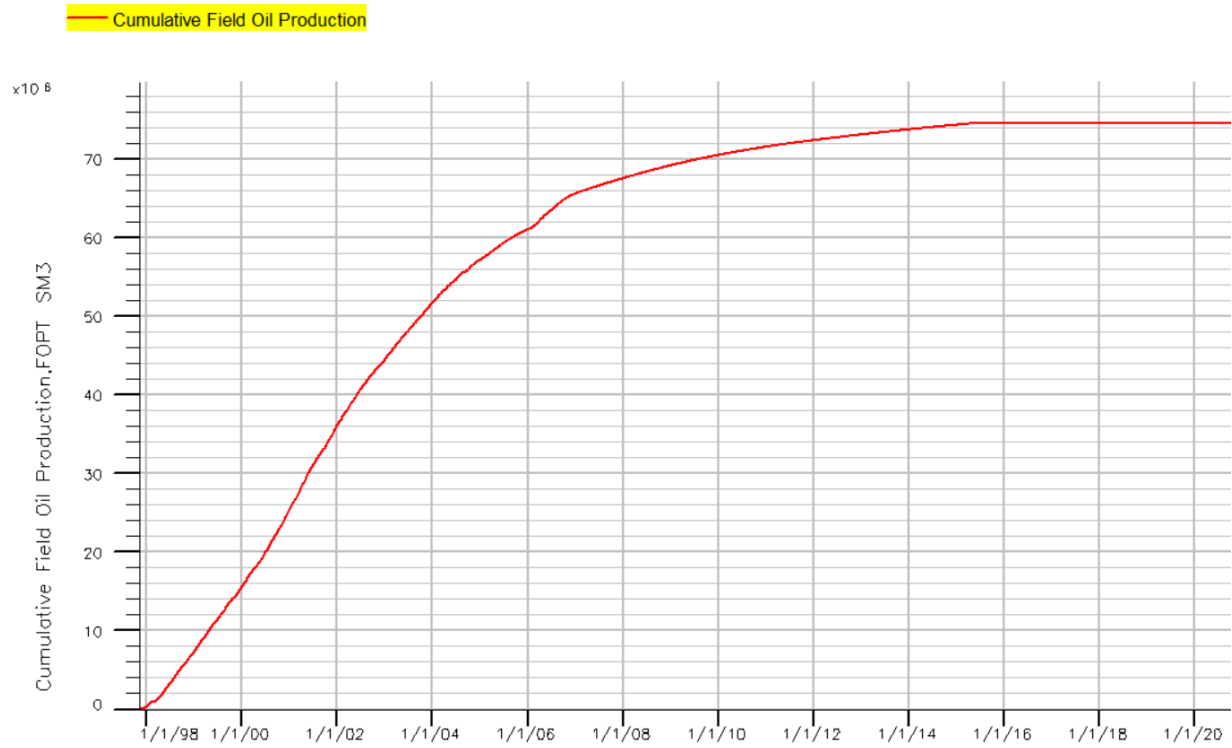


Figure 22 Cumulative Field oil Production Plot

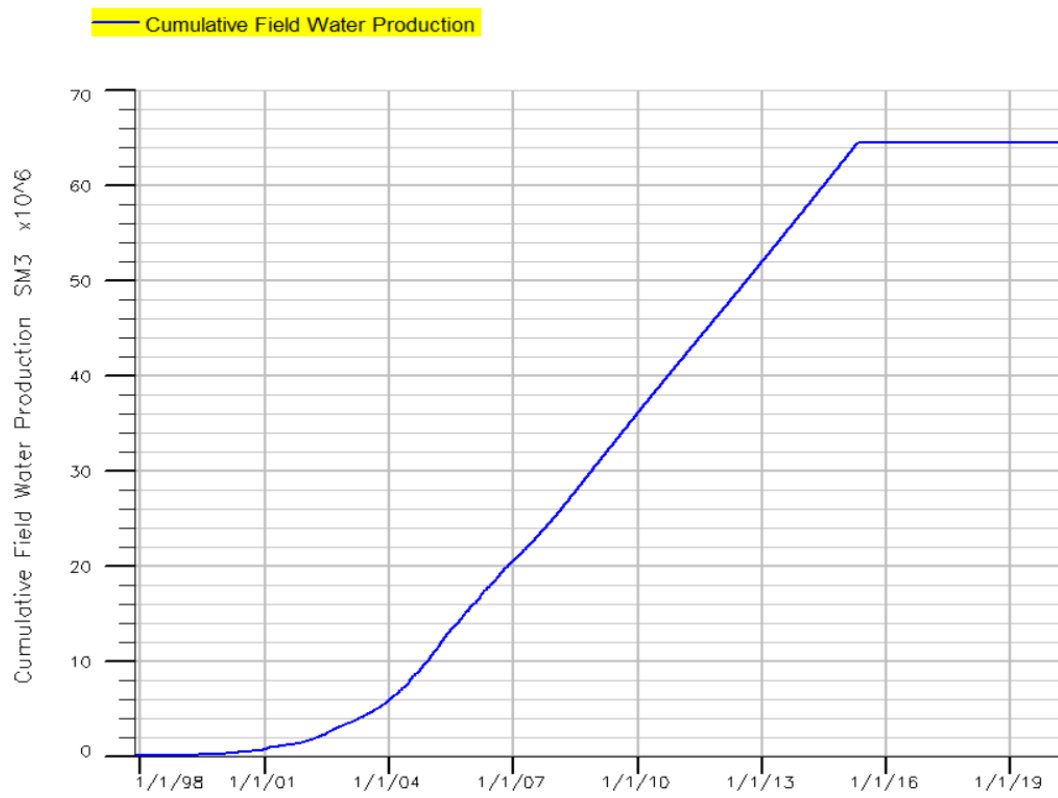


Figure 23 Cumulative Water Production Plot

The Norne field's production and injection history reveal distinct phases that significantly influenced reservoir pressure and fluid dynamics over time. Production began in 1997, and in order to enhance production and maintain reservoir pressure, a water-alternating-gas (WAG) injection strategy was implemented as early as 1998. The cumulative gas and water injection plots below (Fig.24) and (Fig.25), indicate a steady increase in injected volumes, contributing to stable pressure conditions during the early production years.

From 1998 to 2006, WAG injection played a crucial role in maintaining reservoir pressure and optimizing hydrocarbon recovery. However, by 2006, gas injection was discontinued, shifting the pressure maintenance strategy exclusively to water injection. Despite this, the field continued producing oil at declining rates, while cumulative gas production kept rising, indicating a transition to a gas dominated production phase. By 2010, a noticeable pressure decline was observed, reflecting the increasing challenges of reservoir depletion. Water injection continued until 2015, ensuring some degree of pressure support despite declining production efficiency.

Following the cessation of operations, the reservoir pressure stabilized at approximately 130 bar, as indicated by the historical pressure results. The depletion history of the Norne field establishes a favorable setting for hydrogen storage, with stabilized pressure at 120–130 bar providing available pore space for injection. The remaining gas cap offers a suitable medium for storage and the prior WAG injection phase demonstrates that re-pressurization is feasible.

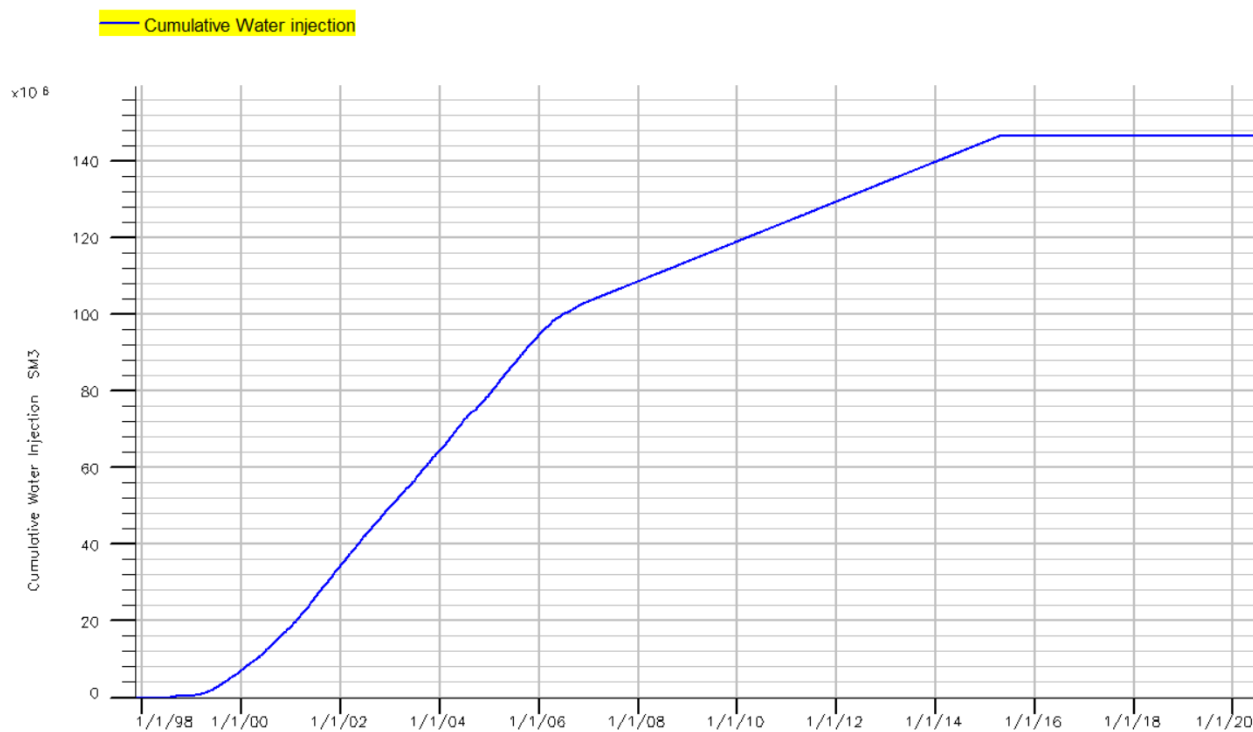


Figure 24 Cumulative Water Injection Plot

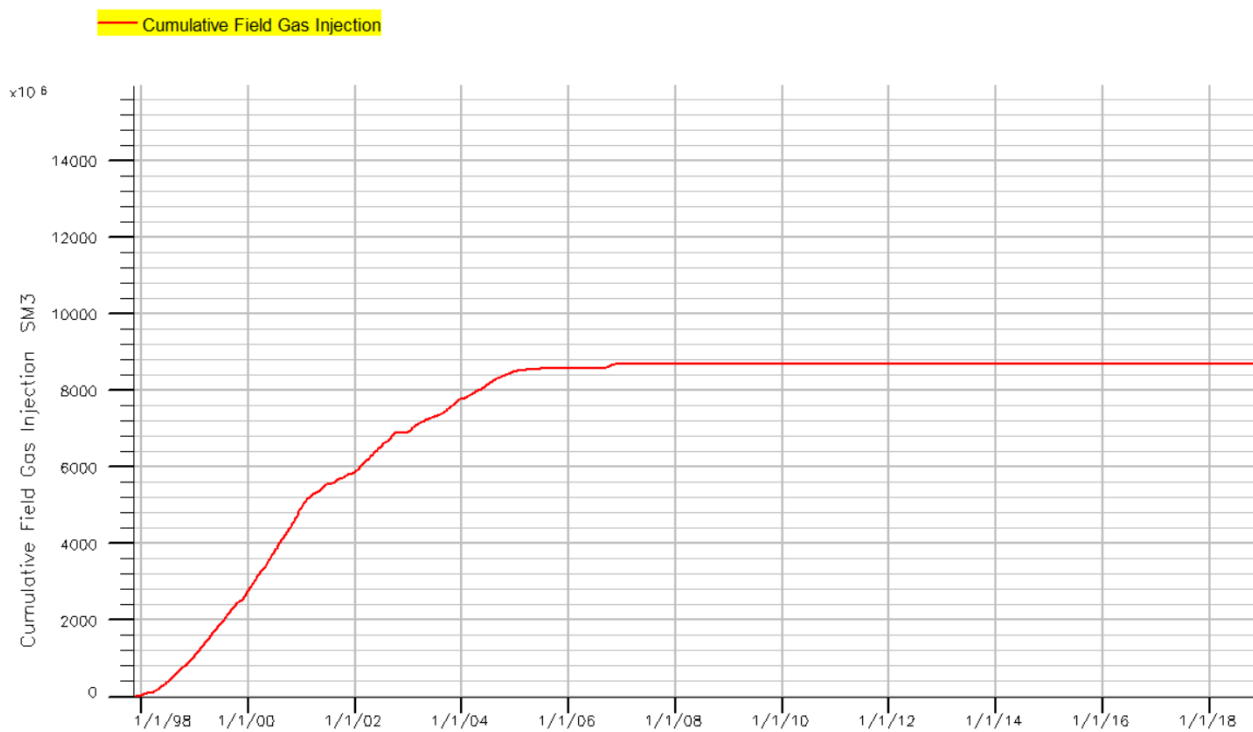


Figure 25 Cumulative Gas Injection Plot

A total of 36 wells have been drilled, of which 8 wells served as injectors and 28 as producers. It is worth pointing out that several wells were used as both injectors and producers. Furthermore, from 1997 (start of production) until 2015, 75 million sm^3 of oil and 25 billion sm^3 of gas have been produced in total. The reservoir's oil and gas originally in place were estimated to be at around 160 million sm^3 and 27 billion sm^3 respectively.

Table 4 Summary of Production and Injection History

<i>Parameter (1997 -2019)</i>	<i>Volume (10^6 msc^3)</i>
<i>OOIP</i>	160
<i>GOIP</i>	27 000
<i>Cumulative oil production</i>	75
<i>Cumulative gas production</i>	25 000
<i>Cumulative water production</i>	65
<i>Cumulative gas Injection</i>	9 000
<i>Cumulative Water Injection</i>	146

To provide a clearer representation of the Norne field's development and well configurations, the figure below (Fig. 26), displays the static model grid, highlighting the locations of all the wells used throughout the production and WAG injection phases. By visualizing the distribution of wells and their relationship with the gas cap and oil-bearing formations, this figure facilitates a more comprehensive assessment of the field's suitability for large-scale underground hydrogen storage applications.

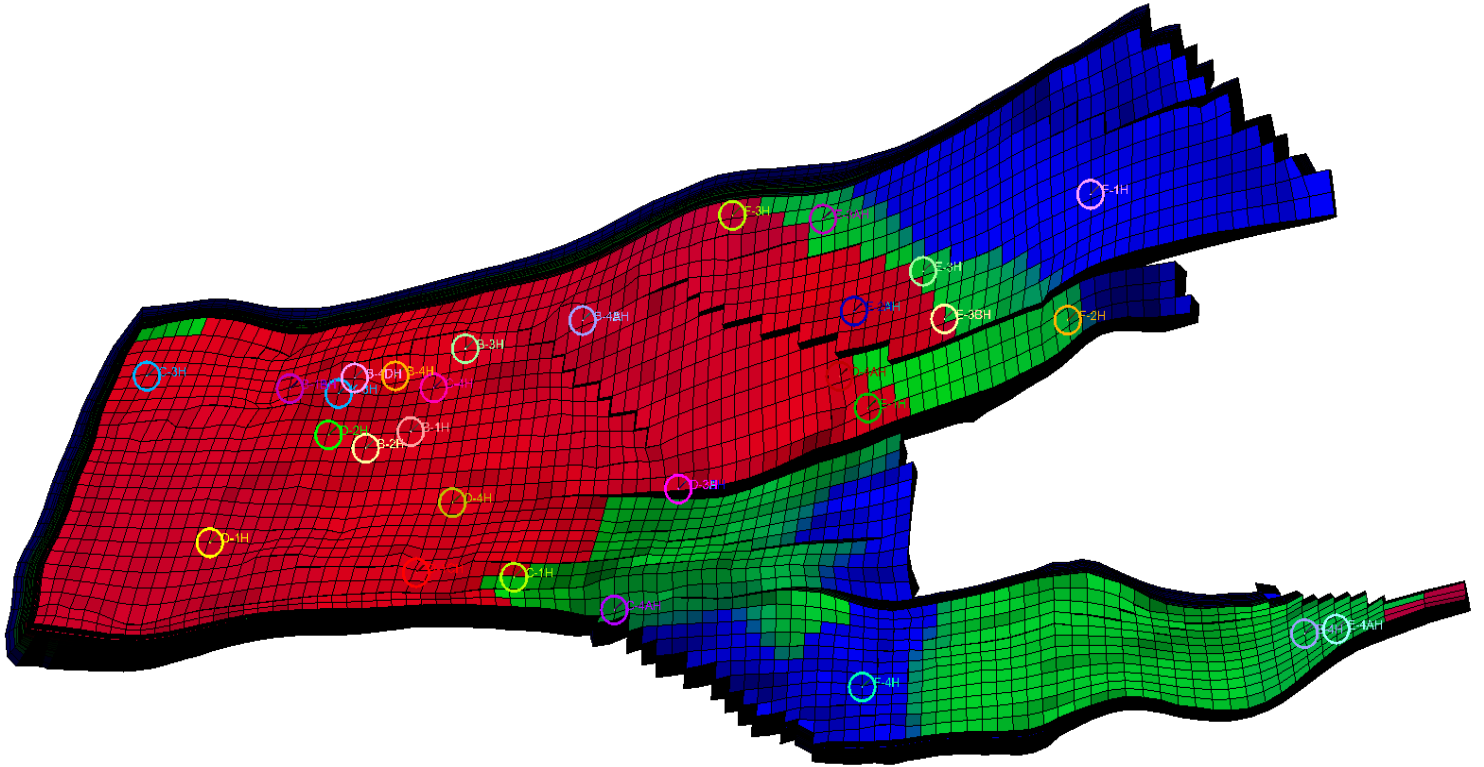


Figure 26 Well distribution map.

3.2.Forecast Scenarios for H₂ Storage

Three different forecast scenarios were tested, each varying in well configuration and operational rates, as summarized in the table below. The existing infrastructure of the Norne field was leveraged by reusing pre-existing wells, some of which were originally injectors, while others were producers during hydrocarbon production. These wells were repurposed for hydrogen injection and withdrawal within the gas cap, optimizing the use of available resources to assess the feasibility of underground hydrogen storage.

Table 5 Summary of Injection and Production Strategies

	Base Case	Case 1	Case 2
Well Configuration	Single well	Eight wells	Eight wells
Injection Rate per well (Sm³/day)	3 000 000	750 000	4 000 000 (infilling phase: 1 000 000)
Total Injection Rate (Sm³/day)	3 000 000	6 000 000	32 000 000 (infilling phase: 8 000 000)
Production Rate per well (Sm³/day)	3 000 000	1 000 000	4 000 000
Total Production Rate (Sm³/day)	3 000 000	8 000 000	32 000 000
Infilling Phase Total Gas Injected Volume (10⁶ msc³)	2405	16125	19050

The Base Case involves injecting and withdrawing hydrogen from a single well at 3 million Sm³/day, aimed at assessing storage feasibility with minimal well infrastructure. Case 1 distributes injection across eight wells resulting in a total injection rate of 6 million Sm³/day and a total production rate of 8 million Sm³/day, while Case 2 follows the same multi-well injection configuration but increases both injection and withdrawal rates to a total of 32 million Sm³/day each. In Case 2 however, during the infilling period, the injection rate was initially set at 1 million Sm³/day per well (total 8 million Sm³/day) instead of the total cyclic rate of 32 million Sm³/day to control the injection and prevent rapid pressure buildup, ensuring a gradual stabilization before cyclic storage began and reducing the risk of exceeding the initial reservoir pressure of 270 bar too quickly. This case was done to determine the effects of high injection and production rates on storage balance and stability. (Fig.27) and (Fig.28) illustrate the variations in injection and

withdrawal rates across the three cases, showing the distinct patterns based on well count and flow rates.

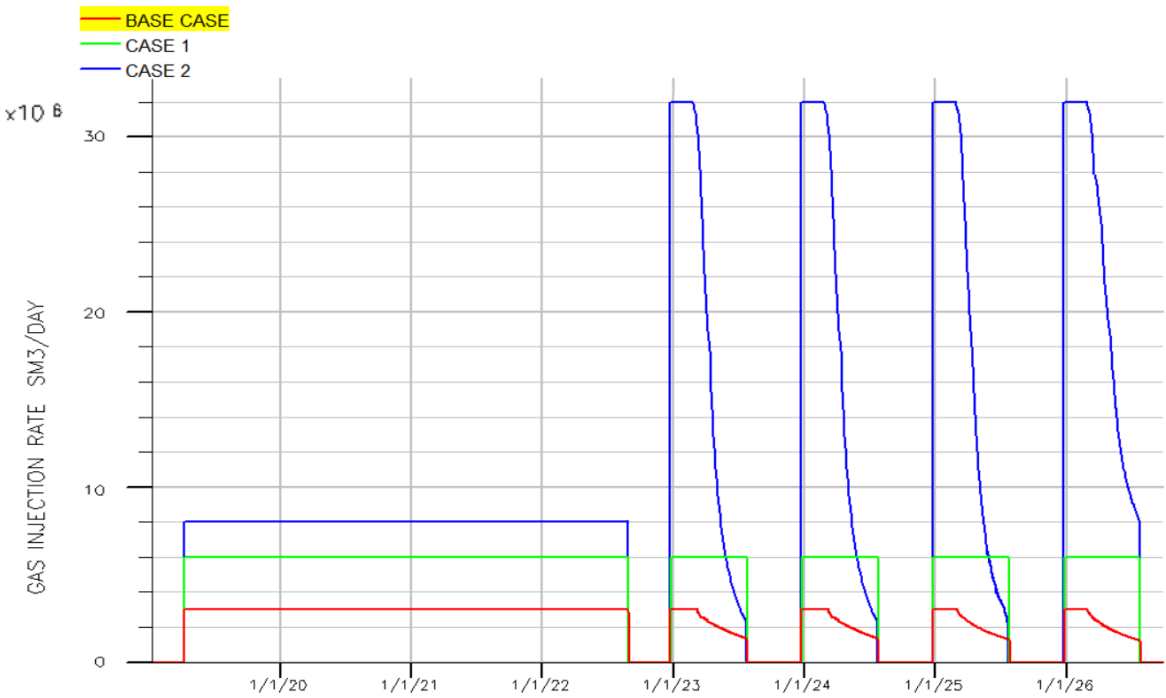


Figure 27 Gas Injection Rates for different scenarios during infilling and storage cycles

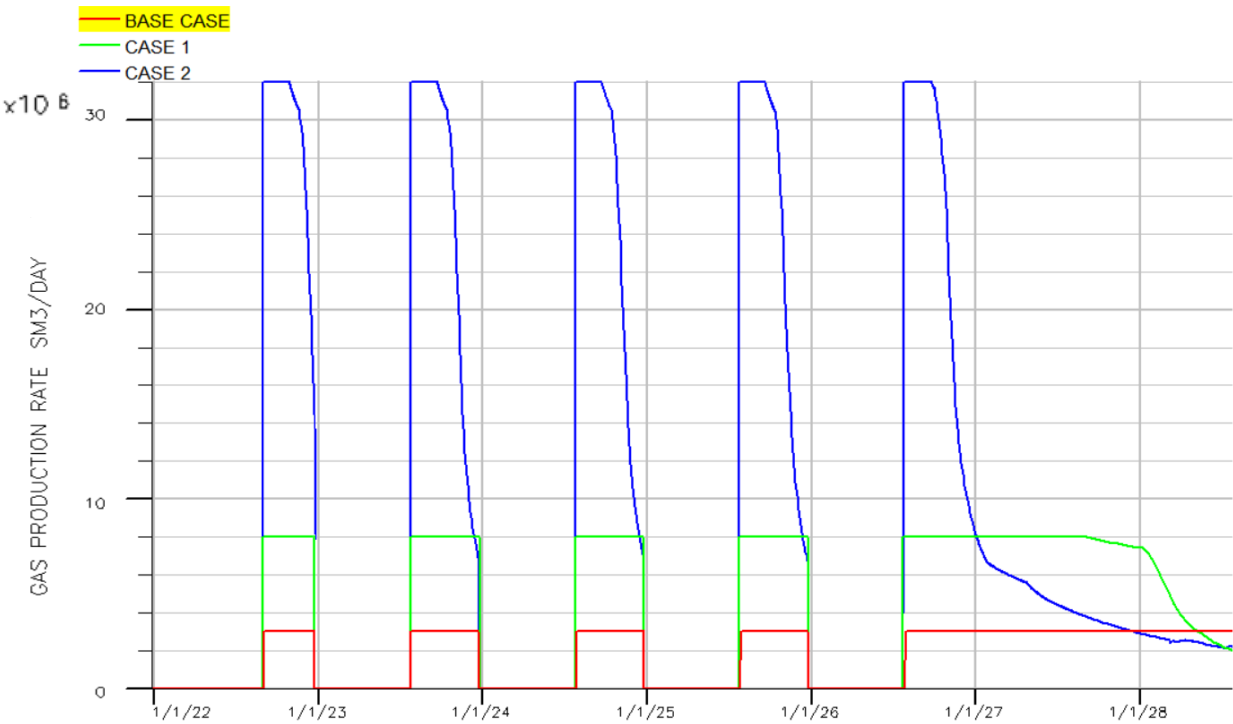


Figure 28 Gas Production Rate variations for different scenarios during withdrawal phases.

3.3.Results and Discussion

The pressure behavior across the three cases provides valuable insights into how different injection and production rates influence pressure stability, gas retention, and overall reservoir performance.

The Plot (Fig.29) below illustrates the regional pressure variations within the gas cap throughout the 10-year storage simulation period, highlighting the effects of injection and withdrawal rates on reservoir conditions.

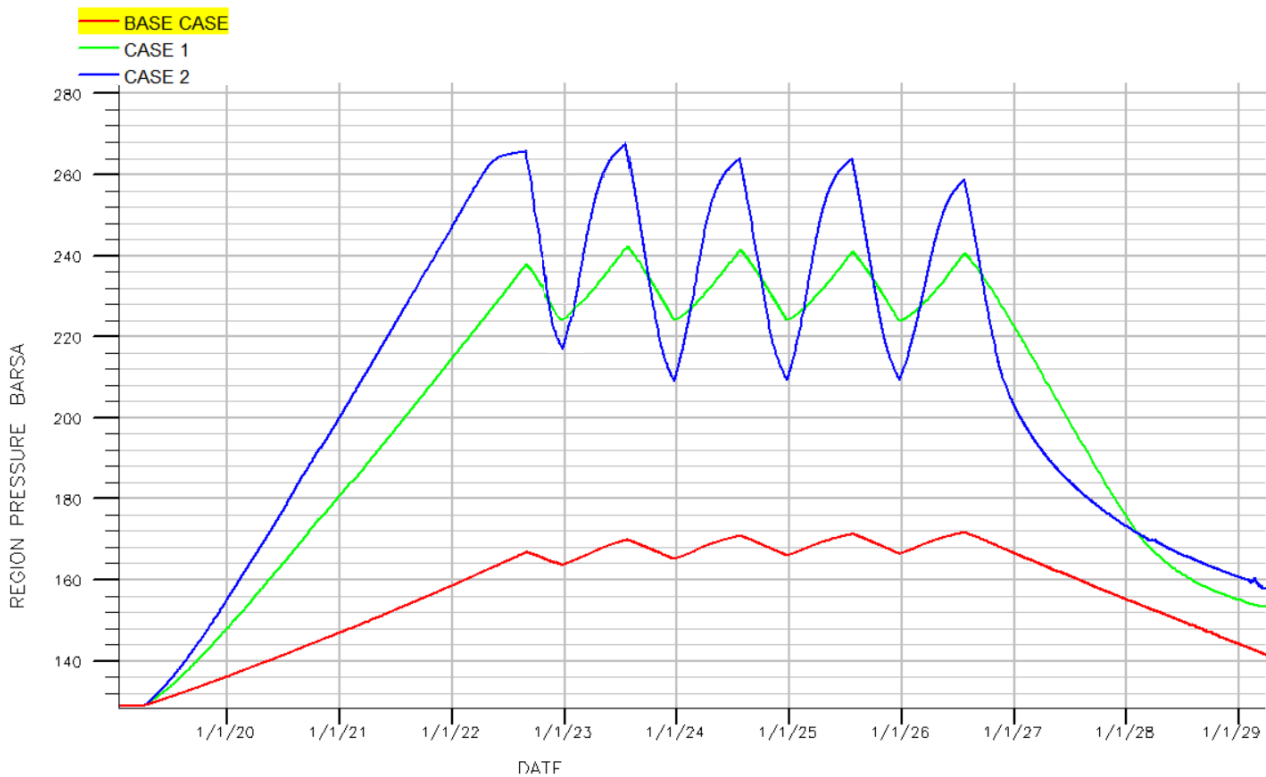


Figure 29 Gas cap regional pressure profile for different storage cases.

During cyclic storage, the Base Case with a single well injecting and producing at 3 million Sm³/day, exhibits the lowest pressure fluctuations, with gradual increases during injection and controlled declines during withdrawal. The lower injection and production volumes ensure a stable

pressure profile with minimal fluctuations but limit storage capacity. In Case 1, where injection and withdrawal points are distributed across eight wells, shows moderate pressure variations, reaching a peak of 245 bar. Pressure remains relatively stable throughout cycles, with controlled declines after each withdrawal phase, indicating better pressure dissipation and storage efficiency compared to the Base Case. Case 2 however, which is subject to the highest injection and withdrawal rates (32 million Sm³/day), experiences extreme pressure swings, with rapid increases during injection, peaking near the initial gas cap regional pressure of 270 bar, followed by steep pressure drops during withdrawal. These fluctuations suggest that higher withdrawal rates cause more aggressive depletion, potentially causing challenges in managing high-rate hydrogen storage, where rapid pressure shifts could lead to fracture propagation and pose operational risks.

During the prolonged withdrawal phase at the end of the cycles, where hydrogen is continuously withdrawn for two years, all cases show a gradual pressure decline, but Case 2 exhibits the sharpest drop which reinforces concerns about rapid depletion effects on gas recovery. Case 1 maintains a more balanced pressure decrease, confirming its effectiveness in sustaining stable production without excessive pressure loss.

The results summarized in the table below emphasize the direct correlation between injection/withdrawal rates and pressure stability. While the higher injection and production rates in Case 2 allow for greater gas throughput, they also introduce the largest pressure swings, making reservoir management more challenging. Case 1 offers a more balanced approach, where injection and production rates are moderate enough to maximize storage capacity while maintaining pressure fluctuations within a manageable range. The Base Case, despite being the most stable, significantly underutilizes the available storage volume due to its lower injection and production rates.

Table 6 Comparison of Pressure Behavior Across Different Cases

Case	Pressure Range (bar)	Pressure Variation During Cycles	Stability and Operational Considerations
Base case (Single-well)	164 – 174	<ul style="list-style-type: none"> Minimal fluctuations Gradual pressure increases and decline 	<ul style="list-style-type: none"> Low storage capacity Highly stable Underutilized reservoir potential
Case 1 (8 wells, moderate rate)	225 – 245	<ul style="list-style-type: none"> Moderate and smooth injection and withdrawal pattern 	<ul style="list-style-type: none"> Balanced storage capacity Reduced localized stress on the reservoir and caprock compared to case 2
Case 2 (8 wells, high rate)	210 – 270	<ul style="list-style-type: none"> High fluctuations Steep pressure spikes and drops 	<ul style="list-style-type: none"> High storage capacity Near caprock pressure limits, risking fracture propagation Aggressive depletion may reduce gas recovery efficiency

Moreover, the gas in place is a critical indicator of reservoir storage performance, reflecting the ability of the formation to retain, cycle, and release injected hydrogen efficiently. The behavior of H₂ in place directly correlates with reservoir pressure dynamics, gas mobility, and production feasibility, making it an essential parameter in evaluating the effectiveness of underground hydrogen storage (UHS). (Fig.30), exhibits the evolution of hydrogen in place across different cases, highlighting how reservoir response changes based on well configuration and injection/withdrawal rates. To quantify these trends, the table below summarizes the injected hydrogen, produced hydrogen, and recovery factor across all cycles.

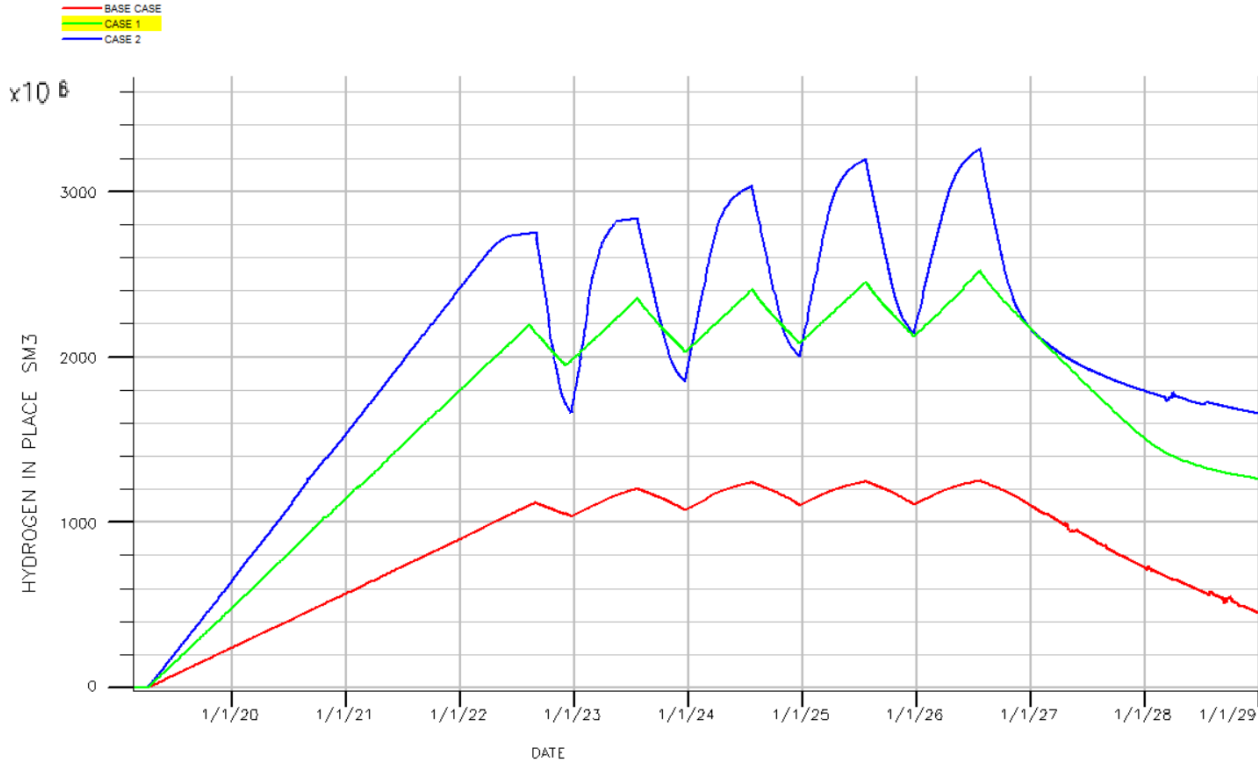


Figure 30 Hydrogen in Place Plot

Case 1 proves to be the optimum scenario, achieving consistently high recovery while maintaining stable storage volumes, suggesting that moderate multi-well injection optimizes gas mobility and reduces retention losses. In contrast, Case 2 exhibits higher peak recovery values but also greater fluctuations in storage stability, indicating that aggressive injection and production rates may introduce operational challenges such as gas redistribution and localized trapping effects. The Base Case, with its single-well injection approach, shows to be the most balanced and stable storage scenario, but having the lowest overall efficiency, it demonstrates that limited capacity restricts gas injectivity and withdrawal, leading to a lower cumulative recovery.

Table 7 Hydrogen Working Gas, Injected Gas, and Recovery Efficiency Across Cycles

Case	Cycles	Working gas (10 ⁶ msc ³)	Injected Gas (10 ⁶ msc ³)	H ₂ Recovery (%)
Base Case	Cycle 1	50	150	33.33
	Cycle 2	120	170	70.58
	Cycle 3	122	172	70.93
	Cycle 4	123	173	70.52

Case 1	Cycle 1	252	400	62.5
	Cycle 2	300	350	85
	Cycle 3	300	351	85
	Cycle 4	300	351	85

Case 2	Cycle 1	1100	1150	95
	Cycle 2	850	1190	79
	Cycle 3	1040	1200	86
	Cycle 4	1050	1100	95

The cumulative hydrogen production plot (Fig.31) displays the total volume of hydrogen extracted over time for each scenario by the end of the two-year withdrawal period. The base case, yielded the lowest production, reaching approximately 1.2 billion Sm³ by the end of the cycles due to its limited withdrawal capacity. In contrast, Case 1 produced around 2.5 billion Sm³, benefiting from a more distributed withdrawal process that improved gas accessibility. On the other hand, Case 2, which operated at the highest injection and production rates, resulted in the largest cumulative hydrogen production, exceeding 5 billion Sm³. However, as previously discussed, the sharp increases in production observed in this scenario suggest the potential for pressure

fluctuations leading to increased stress on the reservoir rock, which could enhance fault reactivation or contribute to fracture propagation.

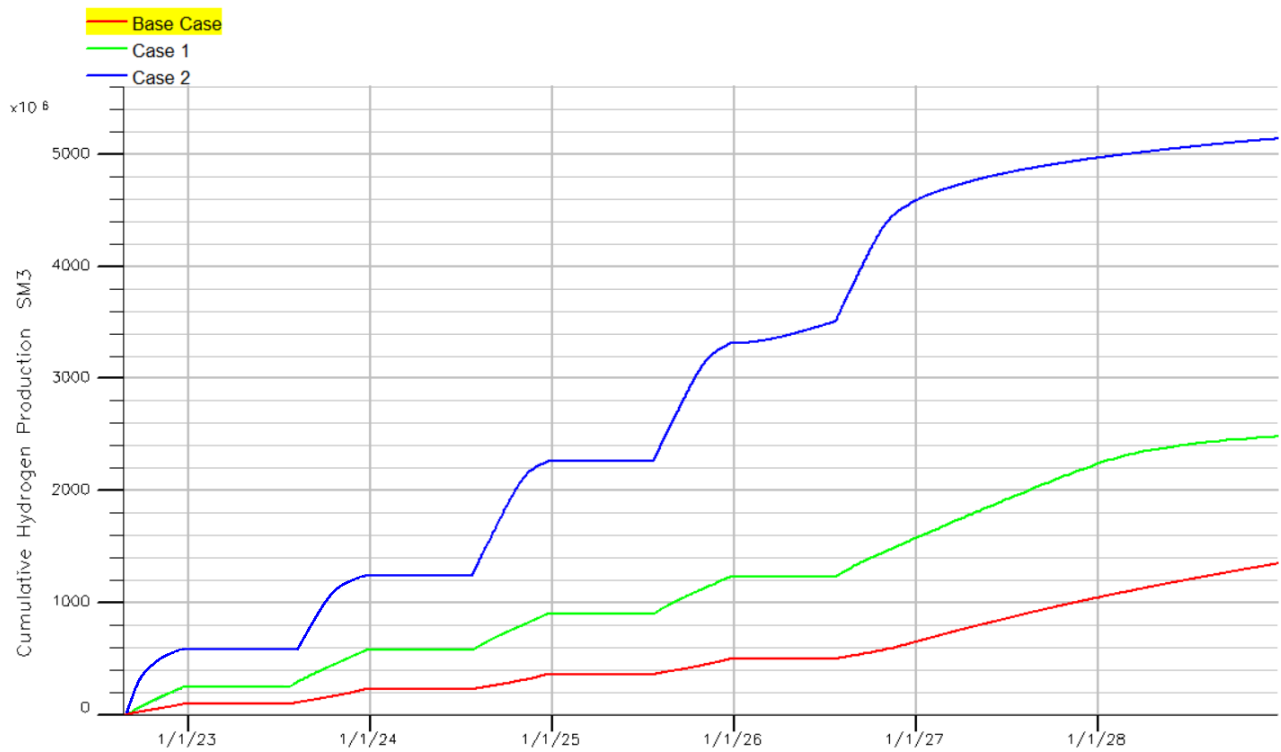


Figure 31 Cumulative H₂ Production Plot

To further understand the spatial distribution of hydrogen within the reservoir, the three figures (Fig.32), (Fig.33), and (Fig.34) below, captured from Petrel after running the dynamic simulation, exhibit H₂ displacement behavior immediately before the injection phase of the third cycle for each of the three cases. On the other hand, figures (Fig.35), (Fig.36), and (Fig.37) demonstrate the H₂ displacement behavior after the injection period is completed, also for each of the three cases.

H_2 saturation distribution in the third cycle before injection for each of the three cases:

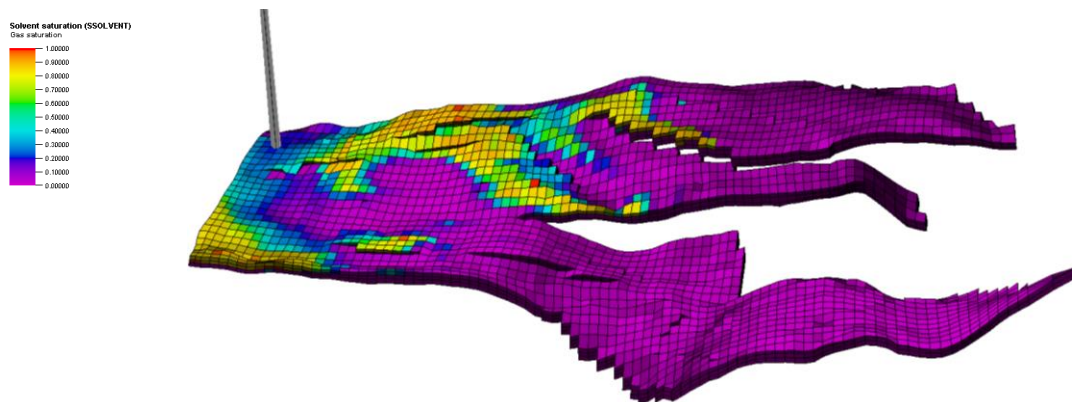


Figure 32 Base Case 3D Grid After Injection

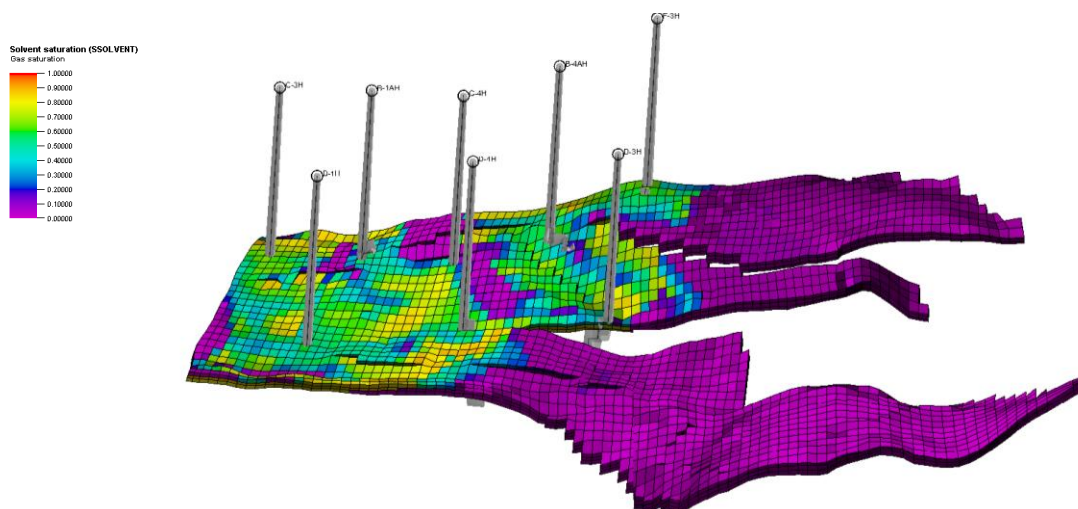


Figure 33 Case 1 3D Grid After Injection

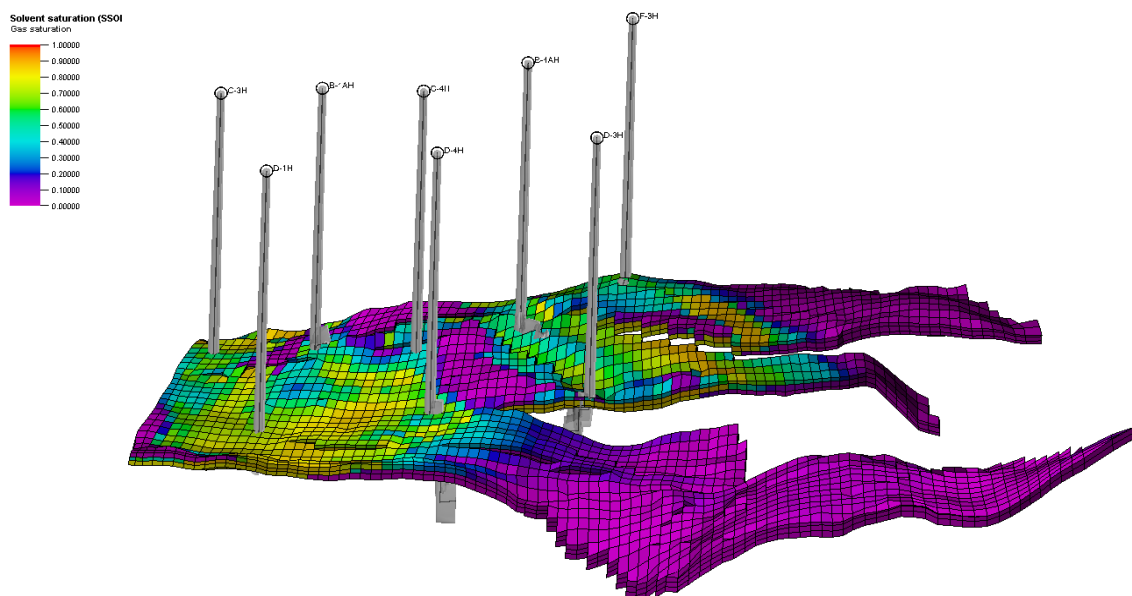


Figure 34 Case 2 3D Grid After Injection

H_2 saturation distribution in the third cycle after injection for each of the three cases:

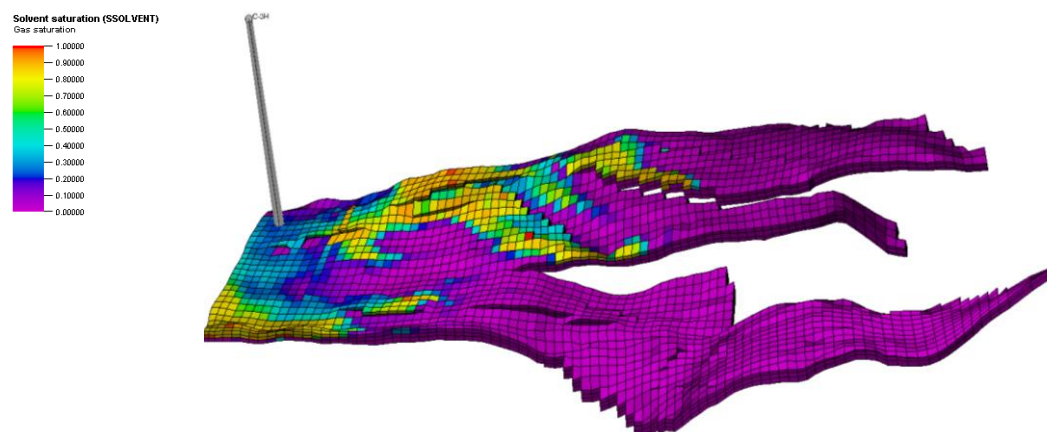


Figure 35 Base Case 3D Grid After Injection

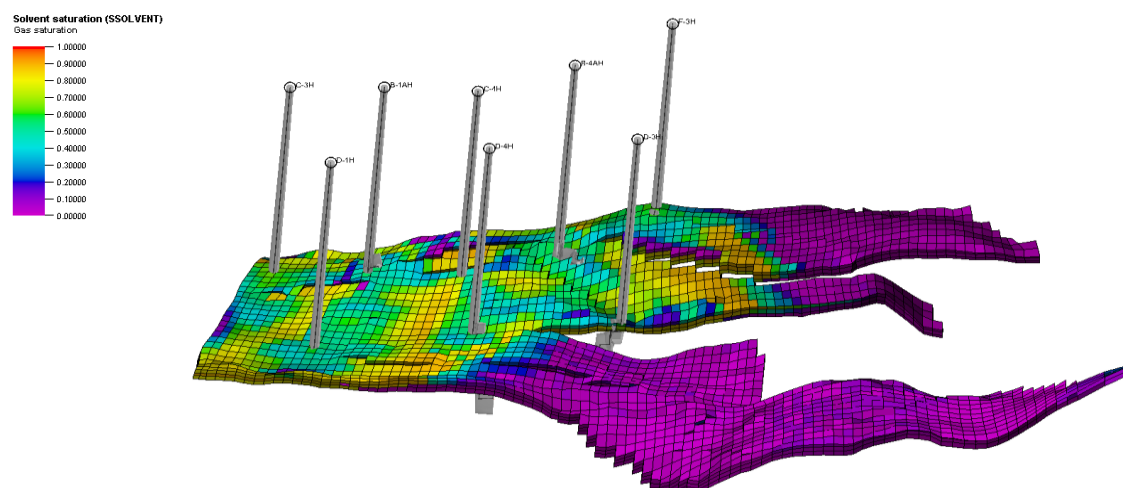


Figure 36 Case 1 3D Grid After Injection

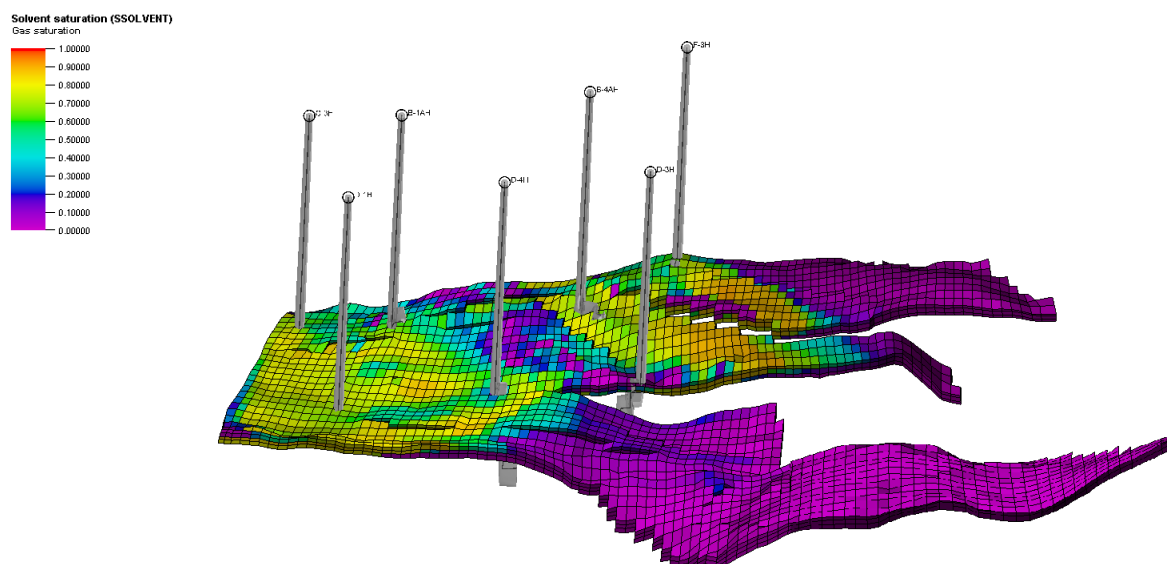


Figure 37 Case 2 3D Grid After Injection

In the Base Case, where a single well is used for injection and withdrawal, hydrogen remains highly localized around the well, leading to poor lateral spread compared to the other and inefficient utilization of the gas cap, compared with the other forecast scenarios. The lack of multiple injection points limits gas displacement, resulting in low volumetric efficiency and restricted storage capacity. Case 1, utilizing eight wells at moderate injection and withdrawal rates, significantly improves hydrogen distribution, ensuring a more uniform spread across the gas cap. This configuration maximizes storage volume utilization, preventing excessive gas retention near injection points and allowing for better hydrogen mobility within the intended storage zone. On the other hand, in Case 2, where the highest injection and withdrawal rates are applied across the same multi-well setup, hydrogen spreads beyond the designated gas cap region, indicating a risk of uncontrolled gas migration. The aggressive injection dynamics force hydrogen to migrate into lower-permeability zones or areas outside the intended storage region, reducing effective storage efficiency and potentially complicating long-term containment and withdrawal operations. While this case maximizes hydrogen volumes, the excessive pressure buildup and saturation imbalance introduce storage instability.

Comparing all scenarios, the Base Case fails to fully utilize the storage potential, while Case 2, despite achieving the highest injection rates, risks hydrogen movement beyond the intended gas cap. Case 1 emerges as the optimal scenario, providing effective hydrogen spread, controlled gas displacement, and stable storage conditions, making it the most suitable strategy for large-scale underground hydrogen storage in the Norne Field.

IV. Conclusion

This study demonstrated the feasibility of repurposing the Norne field for underground hydrogen storage through comprehensive static and dynamic modeling. The static model confirmed that the reservoir's porosity, permeability, and caprock integrity provide a suitable environment for hydrogen injection and withdrawal, while the dynamic simulations evaluated different storage strategies, highlighting their impact on gas distribution, pressure stability, and recovery efficiency. The Base Case, with a single injection and production well, maintained stable pressure conditions but underutilized the reservoir, leading to localized hydrogen accumulation and inefficient displacement. In contrast, Case 1, using eight wells with moderate injection and withdrawal rates, achieved better volumetric sweep, improved hydrogen mobility, and higher recovery efficiency, ensuring a more balanced and stable storage process. Case 2, with the highest injection and withdrawal rates, maximized storage capacity but introduced extreme pressure variations, potential gas migration risks, and operational challenges that could impact long-term stability. The pressure, Gas in Place results and saturation distribution maps confirmed that Case 1 provided the best balance between storage efficiency, recovery potential, and operational stability, making it the most suitable strategy for large-scale hydrogen storage in the Norne field.

Overall, this study confirms that the Norne field can serve as a viable UHS site, with Case 1 emerging as the most efficient and balanced strategy. The findings emphasize the importance of optimizing well placement and injection rates to maximize hydrogen storage while ensuring operational stability.

While this study successfully demonstrates the feasibility of underground hydrogen storage (UHS) in a depleted gas reservoir using a black oil model with solvent tracking, further

investigations and research could benefit from a compositional approach to achieve a more detailed representation of the underlying physical and chemical processes. A fully compositional reservoir simulator would allow for a more precise description of hydrogen solubility in formation water, molecular diffusion, multi-component gas interactions, and geochemical reactions that may influence storage performance over time. Hence, incorporating compositional modeling ensures a more robust evaluation of storage integrity and efficiency in real-world UHS projects.

References

1. International Energy Agency. (2024). *Global hydrogen review 2024*. International Energy Agency. <https://iea.blob.core.windows.net/assets/89c1e382-dc59-46ca-aa47-9f7d41531ab5/GlobalHydrogenReview2024.pdf>
2. International Renewable Energy Agency (IRENA). (2019). *Hydrogen: A renewable energy perspective*. Retrieved from https://www.irena.org/-/media/Files/IRENA/Agency/Publication/2019/Sep/IRENA_Hydrogen_2019.pdf
3. Hassan, Q., Algburi, S., Sameen, A. Z., & others. (2024). Hydrogen as an energy carrier: Properties, storage methods, challenges, and future implications. *Environmental Systems and Decisions*, 44(4), 327–350. <https://doi.org/10.1007/s10669-023-09932-z>
4. U.S. Department of Energy. (2023). *Hydrogen as a clean, flexible energy carrier*. <https://www.energy.gov/eere/articles/hydrogen-clean-flexible-energy-carrier>
5. Tarkowski, R. (2019). *Underground hydrogen storage: Characteristics and prospects*. *Renewable and Sustainable Energy Reviews*, 105, 86–94. <https://doi.org/10.1016/j.rser.2019.01.051>
6. Ammari, H. D., Al-Otaibi, Y. D., & Ammari, T. H. (2021). Hydrogen storage technologies and underground storage options: A review. *Journal of Energy Storage*, 40, 102760. <https://doi.org/10.1016/j.est.2021.102760>
7. Harati, S., Gomari, S. R., Gasanzade, F., Bauer, S., Pak, T., & Orr, C. (2023). Underground hydrogen storage to balance seasonal variations in energy demand: Impact of well configuration on storage performance in deep saline aquifers. *International Journal of Hydrogen Energy*, 48(69), 26894–26910. <https://doi.org/10.1016/j.ijhydene.2023.03.363>
8. He, J., Wang, J., Yu, Q., Cheng, C., & Milsch, H. (2022). Stress-Dependent permeability of naturally Micro-Fractured shale. *Geosciences*, 12(4), 150. <https://doi.org/10.3390/geosciences12040150>
9. Janjua, A. N., Ali, M., Murtaza, M., Patil, S., & Kamal, M. S. (2024). Effects of salinity, temperature, and pressure on H₂–brine interfacial tension: Implications for underground hydrogen storage. *Journal of Energy Storage*, 95, 112510. <https://doi.org/10.1016/j.est.2024.112510>

10. Oni, B. A., Bade, S. O., Sanni, S. E., & Oyinkepreye David Orodu. (2024). Underground hydrogen storage in salt caverns: Recent advances, modeling approaches, barriers, and future outlook. *Journal of Energy Storage*, 107, 114951–114951. <https://doi.org/10.1016/j.est.2024.114951>
11. Haddad, P.G.; Ranchou-Peyruse, M.; Guignard, M.; Mura, J.; Casteran, F.; Ronjon-Magand, L.; Sénéchal, P.; Isaure, M.P.; Moonen, P.; Hoareau, G.; et al. Geological storage of hydrogen in deep aquifers – an experimental multidisciplinary study. *Energy Environ. Sci.* 2022, 15, 3400–3415. <https://doi.org/10.1039/D2EE00765G>
12. A. Amann-Hildenbrand, B.M. Krooss, Harrington, J., R. Cuss, Davy, C., Skoczylas, F., E. Jacobs, & Maes, N. (2015). Gas Transfer Through Clay Barriers. *Developments in Clay Science*, 227–267. <https://doi.org/10.1016/b978-0-08-100027-4.00007-3>
13. Tarkowski, R., & Uliasz-Misiak, B. (2022). Towards underground hydrogen storage: A review of barriers. *Renewable and Sustainable Energy Reviews*, 162, 112451. <https://doi.org/10.1016/j.rser.2022.112451>
14. Gholami, R., Raza, A., & Iglauer, S. (2021). Leakage risk assessment of a CO₂ storage site: A review. *Earth-Science Reviews*, 223, 103849. <https://doi.org/10.1016/j.earscirev.2021.103849>
15. Sainz-Garcia, A., Abarca, E., Rubi, V., & Grandia, F. (2017). Assessment of feasible strategies for seasonal underground hydrogen storage in a saline aquifer. *International Journal of Hydrogen Energy*, 42(26), 16657–16666. <https://doi.org/10.1016/j.ijhydene.2017.05.076>
16. Lysyy, M., Ersland, G., & Fernø, M. (2022). Pore-scale dynamics for underground porous media hydrogen storage. *Advances in Water Resources*, 163, 104167. <https://doi.org/10.1016/j.advwatres.2022.104167>
17. Ali, M., Arif, M., Sahito, M. F., Al-Anssari, S., Keshavarz, A., Barifcani, A., Stalker, L., Sarmadivaleh, M., & Iglauer, S. (2019). CO₂-wettability of sandstones exposed to traces of organic acids: Implications for CO₂ geo-storage. *International Journal of Greenhouse Gas Control*, 83, 61–68. <https://doi.org/10.1016/j.ijggc.2019.02.002>
18. Wolff-Boenisch, D., Wenau, S., Gislason, S. R., & Oelkers, E. H. (2011). Dissolution of basalts and peridotite in seawater, in the presence of ligands, and CO₂: Implications for mineral sequestration of carbon dioxide. *Geochimica Et Cosmochimica Acta*, 75(19), 5510–5525. <https://doi.org/10.1016/j.gca.2011.07.004>

19. Janjua, A. N., Ali, M., Murtaza, M., Patil, S., & Kamal, M. S. (2024). Effects of salinity, temperature, and pressure on H₂–brine interfacial tension: Implications for underground hydrogen storage. *Journal of Energy Storage*, 95, 112510.
<https://doi.org/10.1016/j.est.2024.112510>
20. Salami, B. A., Gbadamosi, A., Adamu, H., Usman, J., Usman, A. G., Jibril, M. M., Ganiyu Kayode Otukogbe, & Abba, S. I. (2023). *Interfacial Tension of the H₂-Brine Modelling Effect on Energy Transition of Hydrogen Geological Storage: Artificial Intelligence Predictive Insights*. <https://doi.org/10.2139/ssrn.4538131>
21. Iglauer, S., Ali, M., & Keshavarz, A. (2021). Hydrogen Wettability of Sandstone Reservoirs: Implications for Hydrogen Geo-Storage. *Geophysical Research Letters*, 48(3). <https://doi.org/10.1029/2020gl090814>
22. CARDEN, P., & PATERSON, L. (1979). Physical, chemical and energy aspects of underground hydrogen storage. *International Journal of Hydrogen Energy*, 4(6), 559–569. [https://doi.org/10.1016/0360-3199\(79\)90083-1](https://doi.org/10.1016/0360-3199(79)90083-1)
23. Nazari, F., Nafchi, S. A., Asbaghi, E. V., Farajzadeh, R., & Niasar, V. J. (2023). Impact of capillary pressure hysteresis and injection-withdrawal schemes on performance of underground hydrogen storage. *International Journal of Hydrogen Energy*, 50, 1263–1280. <https://doi.org/10.1016/j.ijhydene.2023.09.136>
24. Lysyy, M., Føyen, T., Johannesen, E. B., Fernø, M., & Ersland, G. (2022). Hydrogen relative permeability hysteresis in underground storage. *Geophysical Research Letters*, 49(17). <https://doi.org/10.1029/2022gl100364>
25. Hemme, C.; Van Berk, W. Hydrogeochemical Modeling to Identify Potential Risks of Underground Hydrogen Storage in Depleted Gas Fields. *Appl. Sci.* 2018, 8, 2282. <https://doi.org/10.3390/app8112282>
26. Pan, B., Yin, X., Ju, Y., & Iglauer, S. (2021). Underground hydrogen storage: Influencing parameters and future outlook. *Advances in Colloid and Interface Science*, 294, 102473. <https://doi.org/10.1016/j.cis.2021.102473>
27. Rooijen, van, Habibi, P., Xu, K., Dey, P., T. J. H. Vlugt, H. Hajibeygi, & Moulton, O. A. (2023). Interfacial Tensions, Solubilities, and Transport Properties of the H₂/H₂O/NaCl System: A Molecular Simulation Study. *Journal of Chemical & Engineering Data*, 69(2), 307–319. <https://doi.org/10.1021/acs.jced.2c00707>
28. Shi, Z.; Jessen, K.; Tsotsis, T.T. Impacts of the subsurface storage of natural gas and hydrogen mixtures. *Int. J. Hydrog. Energy* 2020, 45, 8757–8773. <https://doi.org/10.1016/j.ijhydene.2020.01.044>.

29. Dopffel, N., Mayers, K., Abduljelil Kedir, Alagic, E., Biwen Annie An-Stepec, Ketil Djurhuus, Boldt, D., Janiche Beeder, & Hoth, S. (2023). Microbial hydrogen consumption leads to a significant pH increase under high-saline-conditions: implications for hydrogen storage in salt caverns. *Scientific Reports*, 13(1).
<https://doi.org/10.1038/s41598-023-37630-y>
30. BUZEK, F., V ONDERKA, VANCURA, P., & WOLF, I. (1994). Carbon isotope study of methane production in a town gas storage reservoir. *Fuel*, 73(5), 747–752.
[https://doi.org/10.1016/0016-2361\(94\)90019-1](https://doi.org/10.1016/0016-2361(94)90019-1)
31. MIGA, P. (1990). Methanogenic bacteria as a key factor involved in changes of town gas stored in an underground reservoir. *FEMS Microbiology Letters*, 73(3), 221–224.
[https://doi.org/10.1016/0378-1097\(90\)90733-7](https://doi.org/10.1016/0378-1097(90)90733-7)
32. Schwab, L., Prinsen, L., Nowack, G., Popp, D., Noll, M., Vogt, C., & Wagner, M. (2023). *Sulfate reduction and homoacetogenesis at various hypersaline conditions: Implications for H₂ underground gas storage. II.*
<https://doi.org/10.3389/fenrg.2023.1125619>
33. Vasile, & Santi Vasile, N. (2024). *POLITECNICO DI TORINO Repository ISTITUZIONALE A Comprehensive Review of Biogeochemical Modeling of Underground Hydrogen Storage: A Step Forward in Achieving a Multi-Scale Approach*
<https://iris.polito.it/retrieve/9273cb1a-8466-417f-9885-ece999ff59d6/energies-17-06094.pdf>
34. Eberle, U., Felderhoff, M., & Schüth, F. (2009). Chemical and physical solutions for hydrogen storage. *Angewandte Chemie International Edition*, 48(36), 6608–6630.
<https://doi.org/10.1002/anie.200806293>
35. Hassanpouryouzband, A., Adie, K., Cowen, T., Thaysen, E. M., Heinemann, N., Butler, I. B., Wilkinson, M., & Edlmann, K. (2022). Geological Hydrogen Storage: Geochemical Reactivity of Hydrogen with Sandstone Reservoirs. *ACS Energy Letters*, 7(7), 2203–2210. <https://doi.org/10.1021/acseenergylett.2c01024>
36. Homoud, R. A., Vitor, M., Daigle, H., & Ates, H. (2025). Critical Geochemical and Microbial Reactions in Underground Hydrogen Storage: Quantifying Hydrogen Loss and Evaluating CO₂ as Cushion Gas. *Hydrogen*, 6(1), 4–4.
<https://doi.org/10.3390/hydrogen6010004>

37. Saeed, M., Jadhawar, P., & Bagala, S. (2023). Geochemical Effects on Storage Gases and Reservoir Rock during Underground Hydrogen Storage: A Depleted North Sea Oil Reservoir Case Study. *Hydrogen*, 4(2), 323–337.
<https://doi.org/10.3390/hydrogen4020023>
38. Flesch, S., Pudlo, D., Albrecht, D., Jacob, A., & Enzmann, F. (2018). Hydrogen underground storage—Petrographic and petrophysical variations in reservoir sandstones from laboratory experiments under simulated reservoir conditions. *International Journal of Hydrogen Energy*, 43(45), 20822–20835.
<https://doi.org/10.1016/j.ijhydene.2018.09.112>
39. Dokhon, W., Goodarzi, S., Alzahrani, H. M., Blunt, M. J., & Bijeljic, B. (2024). Pressure decline and gas expansion in underground hydrogen storage: A pore-scale percolation study. *International Journal of Hydrogen Energy*, 86, 261–274.
<https://doi.org/10.1016/j.ijhydene.2024.08.139>
40. Zeng, L., Vialle, S., Ennis-King, J., Esteban, L., Sarmadivaleh, M., Sarout, J., Dautriat, J., Giwelli, A., & Xie, Q. (2022, September 30). *Role of Geochemical Reactions on Caprock Integrity During Underground Hydrogen Storage*. Social Science Research Network.
<https://doi.org/10.2139/ssrn.4233860>
41. Harati, S., Gomari, S. R., Ramegowda, M., & Pak, T. (2023). Multi-criteria site selection workflow for geological storage of hydrogen in depleted gas fields: A case for the UK. *International Journal of Hydrogen Energy*, 51, 143–157.
<https://doi.org/10.1016/j.ijhydene.2023.10.345>
42. Borello, E. S., Bocchini, S., Chiodoni, A., Coti, C., Fontana, M., Panini, F., Peter, C., Pirri, C. F., Tawil, M., Mantegazzi, A., Marzano, F., Pozzovivo, V., Verga, F., & Viberti, D. (2024). Underground Hydrogen Storage Safety: Experimental Study of Hydrogen Diffusion through Caprocks. *Energies*, 17(2), 394. <https://doi.org/10.3390/en17020394>
43. Editor Engineeringtoolbox. (2024b, April 8). Hydrogen - Thermophysical properties.
https://www.engineeringtoolbox.com/hydrogen-d_1419.html
44. Blunt, M. J. (2016b). *Multiphase flow in permeable media*.
<https://doi.org/10.1017/9781316145098>

45. Heinemann, N., Alcalde, J., Miocic, J. M., Hangx, S. J. T., Kallmeyer, J., Ostertag-Henning, C., Hassanpouryouzband, A., Thaysen, E. M., Strobel, G. J., Schmidt-Hattenberger, C., Edlmann, K., Wilkinson, M., Benthams, M., Haszeldine, R. S., Carbonell, R., & Rudloff, A. (2021b). Enabling large-scale hydrogen storage in porous media – the scientific challenges. *Energy & Environmental Science*, 14(2), 853–864. <https://doi.org/10.1039/d0ee03536j>
46. Jangda, Z., Menke, H., Busch, A., Geiger, S., Bultreys, T., Lewis, H., & Singh, K. (2022). Pore-scale visualization of hydrogen storage in a sandstone at subsurface pressure and temperature conditions: Trapping, dissolution and wettability. *Journal of Colloid and Interface Science*, 629, 316–325. <https://doi.org/10.1016/j.jcis.2022.09.082>
47. Jutila, H. A., Cullen, M., Hayhurst, S., Howell, K., Fullarton, L., Heydari, E., & Orley, M. (2024). Rough Gas Storage Site – Redeveloping and Making it Hydrogen Ready. *SPE Europe Energy Conference and Exhibition*. <https://doi.org/10.2118/220061-ms>
48. Barison, E., Donda, F., Merson, B., Le Gallo, Y., & Réveillère, A. (2023). An Insight into Underground Hydrogen Storage in Italy. *Sustainability*, 15(8), 6886. <https://doi.org/10.3390/su15086886>
49. Richard Wilfred Rwechungura, Eka Suwartadi, Mohsen Dadashpour, Kleppe, J., & Foss, B. A. (2010). *The Norne Field Case—A Unique Comparative Case Study*. <https://doi.org/10.2118/127538-ms>
50. IEA. (2019). *The Future of Hydrogen Seizing today's opportunities*. https://iea.blob.core.windows.net/assets/9e3a3493-b9a6-4b7d-b499-7ca48e357561/The_Future_of_Hydrogen.pdf
51. Abdellatif, M., Hashemi, M., & Azizmohammadi, S. (2023). Large-scale underground hydrogen storage: Integrated modeling of reservoir-wellbore system. *International Journal of Hydrogen Energy*. <https://doi.org/10.1016/j.ijhydene.2023.01.227>
52. Muhammed, N. S., Haq, M. B., Al Shehri, D. A., Al-Ahmed, A., Rahman, M. M., Zaman, E., & Iglauer, S. (2023). Hydrogen storage in depleted gas reservoirs: A comprehensive review. *Fuel*, 337, 127032. <https://doi.org/10.1016/j.fuel.2022.127032>

53. Lan, Y., Guo, P., Liu, Y., Wang, S., Cao, S., Zhang, J., Sun, W., Qi, D., & Ji, Q. (2024). State of the Art on Relative Permeability Hysteresis in Porous Media: Petroleum Engineering Application. *Applied Sciences*, 14(11), 4639–4639.
<https://doi.org/10.3390/app14114639>
54. Akpasi, S. O., Smarte, M., Tetteh, E. K., Ubani Oluwaseun Amune, Mustapha, S. I., & Kiambi, S. L. (2025). Hydrogen as a Clean Energy Carrier: Advancements, Challenges, and its Role in a Sustainable Energy Future. *Clean Energy*.
<https://doi.org/10.1093/ce/zkae112>
55. National Institute of Standards and Technology. (2018). *Thermophysical Properties of Fluid Systems*. Nist.gov. <https://webbook.nist.gov/chemistry/fluid/>
56. OPM | The Open Porous Media Initiative. (2015). Opm-Project.org. <https://opm-project.org/>